# Poly(vinyl alcohol) PVA hydrogel characterization as a potential nucleus pulposus replacement candidate

Chun Ying, Liang

Masters in biomedical engineering

Department of Biomedical Engineering

Department of Biomedical Engineering

McGill University

Montreal, Quebec, Canada

February 18<sup>th</sup>, 2008

A thesis submitted in partial fulfillment of the requirements for the degree in Master of Engineering

©Copyright 2008 All rights reserved.

# Dedication

To my parents,

Ben and Shu Chang Liang

# Acknowledgments

I would like to express my gratitude to those who have been involved in making this project possible. I am greatly indebted to my supervisor Dr. Thomas Steffen, who gave much valuable advice, guidance and encouragement throughout the project. A special thanks goes out to Mr Lorne Beckman, who unconditionally assisted me in the process of designing and machining as required for my experimental setups. To my wonderful laboratory members who had shared my many frustrations and joys, especially to Scott McGrail, who assisted me in my experiments when I had other commitments to attend to. To Demetrios Giannitsios and Bernice Jim, thank you for your support and guidance, as well as directing me along the right path throughout my project. Lastly, to my parents, words of gratitude are not enough to express how much I am indebted to you. Thank you for believing in me.

# **Table Of Contents**

Dedication	ii
Table Of Contents	iv
List Of Tables	vi
List Of Figures	vii
Abstract (English)	1
Abstract (French)	2
Chapter 1: Introduction	3
Chapter 2: Literature Review	5
2.1 Intervertebral disc	5
2.1.1 Biochemistry & function of the intervertebral disc	5
2.1.2 Degenerative disc disease & lower back pain	7
2.2 Current treatments	8
2.2.1 Spinal fusion	9
2.2.2 Disc arthroplasty	10
2.3 Nuclear pulposus replacement & future technologies	11
2.3.1 Intradiscal implants	14
2.3.2 In-situ curing polymer implant	14
2.4 Hydrogels	15
2.4.1 Poly(vinyl alcohol) hydrogel	17
2.5 Hydrogel potential as a NP replacement	18
2.5.1 PVA hydrogel as a NP replacement	19
2.6 Novel PVA hydrogel as an <i>in-situ</i> curing NP replacement candidate	20
2.6.1 Swelling	22
2.6.2 Stiffness	25
2.6.3 Extrusion forces	25
2.6.4 Curing properties	26
2.7 Long term studies	26
2.7.1 Creep and fatigue	26
Chapter 3: Selected Research Approach	29
3.1 Research aims	29
Chapter 4: Material & Methods	31

4.1 PVA hydrogels	31
4.2 Swelling capability	31
4.2.1 Experimental procedure	32
4.3 Unconfined Compression	34
4.3.1 Experimental procedure	34
4.4 Hydrogel extrusion	36
4.4.1 Experimental setup	37
4.4.2 Experimental procedure	40
4.5 Curing Stiffness	45
4.5.1 Specimen selection and preparation	46
4.5.2 Experimental setup	48
4.5.3 Experimental Procedure	51
Chapter 5: Results	56
5.1 Swelling	56
5.2 Unconfined compression	57
5.3 Gel extrusion	61
5.4 Gel Curing	65
Chapter 6: Discussions	70
6.1 PVA hydrogels	70
6.2 Swelling	70
6.3 Unconfined compression	71
6.4 Gel extrusion	73
6.4.1 Experimental design	73
6.4.2 Extrusion volumes	75
6.4.3 Choice of extrusion temperature	76
6.4.4 Extrusion results	76
6.5 PVA hydrogel curing	77
6.5.1 Experimental design rational	78
6.5.2 Hydrogel curing results	79
Chapter 7: Summary & Conclusions	81
Bibliography	83
Appendix	89

# List Of Tables

Table 1: A summary of non-cell seeded nuclear replacements under	
investigation.	.13
Table 2: Screening results of creep experimentation	.28
Table 3: Classification of hydrogels used for the extrusion experiments	.37
Table 4: Relationship between volume, displacement and rate of	
displacement	.41
Table 5: Batch of hydrogel, total number of tubes and moulds required for	
PVA121	.47
Table 6: Batch of hydrogel, total number of tubes and moulds required for	
PVA14X	.47
Table 7 Plateau pressure recordings for PVA121	.63
Table 8: Plateau pressure recordings for PVA14X	.63
Table 9: Thermal conductivity of different materials at 20 °C	.74

# List Of Figures

Figure 1: Grading scheme of age-related disc morphology by Thomspon <i>et al</i> [29]8
Figure 2: a) SB Charité Artificial disc (DePuy Spine), b) Prodisc (Synthes Inc.),
Figure 3: PVA polymerized molecular structure
Figure 4: A breakdown schematic diagram of an injectable hydrogel NP process
Figure 5: Screening results, swelling characterization with different water
content percentage
hydrogels24
Figure 7: Swelling characterization vs. lapsed time after production24
Figure 8: Screening results from hydrogel PVA11627
Figure 9: Slicing setup to cut hydrogel rods into 1:1 height to diameter ratio 33
Figure 10: Schematic diagram of the experimental setup used for hydrogel extrusion
Figure 11: Extrusion syringe with the detachable plunger (Including plunger
stem)
Figure 12: The setup features a) height adjustable disc plate, b) slotted disc
plate,
Figure 13: A flow diagram of the experimental procedure for hydrogel
extrusion43
Figure 14: Boiling waterbath to melt the hydrogel encased in the syringe body
Figure 15: The hydrogel was being extruded from the bottom of the cannula
Figure 16: Brass cast assembly, before and after48
Figure 17: Slotting the thin brass tube with an end-mill of 7/64" width49
Figure 18: a) Longitudinal view of the syringe setup, sealed with a female-end
luer-lock cap, a plunger and metal wire in place, b) Cross-sectional view of
the metal wire locking the Delrin® plunger, c) Delrin® plunger system50
Figure 19: Flow diagram of the experimental procedure to characterize the
curing hydrogel's stiffness over time
Figure 20: Hydrogel locked within a medallion 10 cc syringe, in boiling
waterbath
Figure 21: The entire injection setup, including the syringe, plunger and the
device with a threaded rod and T-handle53
Figure 22: Extrusion of hot hydrogel into the mould connected to a vacuum
pump
,
Figure 24: Swelling ability of PVA121
Figure 25: Swelling ability of PVA14X
Figure 26: Hydrogel specimen before and after an unconfined compression
testing
Figure 27: A Stress vs. Strain during compression of PVA14X at 0 hrs59

Figure 28: Modulus of elasticity for hydrogels plotted for different strain	
intervals of unconfined compression. All tests were performed after swelling	
in 37 °C PBS for different time intervals, except for the controls in 'a'	
Figure 29: Pressure required to extrude hydrogel PVA121 at t = -5 min (100	
°C), t =0 min, 15 min, 30 min, 45 min and 60 min in a 50 °C waterbath	
Figure 30: Regression plot of PVA 121 pressure plateau values over time	
Figure 31: Regression plot of PVA14X pressure plateau/non-plateau values	
	64
Figure 32: a) Encased cured hydrogel b) Cured hydrogel with a sub-optimal	-
shape	
Figure 33: Cured hydrogel removed from its mould	
Figure 34: An example of an air bubble 3 mm in diameter entrapped in a	
·	67
Figure 35: Modulus change of PVA121 measured at 10-20 % strain over a	
period of 2 wks curing. The control value is obtained from a similar hydrogel	l
·,	68
Figure 36: Modulus change of PVA121 measured at 20-30 % strain over a	
period of 2 wks curing. The control value is obtained from a similar hydrogel	
	68
Figure 37: Modulus change of PVA14X measured at 10-20 % strain over a	
period of 2 wks curing. The control value is obtained from a similar hydrogel	
	69
Figure 38: Modulus change of PVA14X measured at 20-30 % strain over a	
period of 2 wks curing. The control value is obtained from a similar hydrogel	l
	69
Figure 39: Cooling rate of water in a make-shift aluminium tube	75
	78
Figure 41: Second prototype of a hydrogel casting mould	79

# Abstract (English)

Chronic lower back pain is a clinical manifestation of vertebral disc degeneration. An emerging technique, nucleoplasty, aims to target early stages of disc degeneration. It is envisioned to inject a liquid-state polymer, poly(vinyl alcohol) hydrogels, into the nuclear cavity and allowed to cure *in-situ*. Two formulations of poly(vinyl alcohol) hydrogels were investigated for its suitability as an injectable polymer. Therefore, its swelling ability, stiffness, required extrusion pressures and temperature dependent curing rates were characterized. Comparable to native nucleus pulposus tissue, the hydrogels swell approximately 10–20 wt% and maintained 1–2.5 MPa stiffness over eight weeks in immersed in phosphate buffer saline. Extrusion pressures highly varied for different hydrogel temperatures and lapsed time. Curing rates for the first hydrogel formulation were slow whereas the second formulation reached within 72 hrs about 70 % of its final cured stiffness. The second hydrogel formulation is a more promising candidate for clinical use.

# Abstract (French)

La lombalgie chronique est la manifestation clinique de la dégénération des disques intervertébraux. La nucleoplastie est une nouvelle technique destinée à traiter la dégénération du disque dans ses premières phases. Le principe consiste à injecter un polymère sous forme liquide, l'hydrogel poly(vinyl alcool), dans le nucléus pulposus, et de le laisser durcir in situ. Deux types d'hydrogels poly(vinyl alcool) ont été étudiés ici pour cette application. La capacité à s'étendre, la rigidité, la pression requise pour l'extrusion et la vitesse de durcissement en fonction de la température ont ainsi été caractérisés pour chacun des deux polymères. Les hydrogels ont des caractéristiques semblables au nucléus pulposus naturel : ils s'étendent de 10 à 20 % en poids et, immergés dans du tampon phosphate salin, maintiennent une rigidité de 1-2.5 MPa pendant 8 semaines. La pression d'extrusion varie significativement avec la température de l'hydrogel et le temps écoulé. La vitesse de durcissement du premier hydrogel était lente, alors que le second atteignait 70 % de sa rigidité finale en moins de 72 heurs. Cette seconde formulation semble plus prometteuse pour des applications cliniques.

## Chapter 1: Introduction

Approximately 8 in every 10 adults will experience some form of lower back pain in their lifetime, of which, 5–10 % of the population will result in chronic disability [1]. It is believed that over 75 % of chronic lower back pain (LBP) results from lumbar disc degeneration [2]. This disabling lower back pain costs the United States approximately 50 billion dollars [2] and the United Kingdom of 12 billion pounds [3].

While the majority of lower back pain patients require only conservative treatment such as per oral pain medication, injection and physiotherapy, patients with persistent unresponsive to conservative treatment cases may eventually require surgery. Till date, spinal fusion is the gold standard for surgery to back relief back pain. However, this surgical method results in the loss of joint motion and increases the risk of future relapse in local and adjacent intervertebral segments. These major drawbacks propelled the development of total disc replacement (disc arthroplasty), nucleus pulposus replacement (nucleoplasty) and other treatment modalities.

Although the exact pathophysiology of degenerative disc disease is still unknown, it is becoming more probable that treatment can be applied during the early stages of disc degeneration, such as to retard disc retarding deterioration, or even reversing disc degeneration in the near future [4]. On such methods can be nucleus pulposus replacement. NP replacement targets earlier stages of disc degeneration in attempt to retard the process of disc degeneration. If the goal of NP replacement can be realised, it may result in a much less invasive and more cost effective surgical procedure compared to spinal fusion surgery.

Hydrogels are a class of three-dimensional polymer networks with water-retaining properties and superior biocompatibility that have been widely utilized in the medical industry since the 1950s [5]. In the past fifteen years, there has been much interest to utilize these hydrogels for a NP replacement.

Poly(vinyl alcohol), PVA, hydrogels are very biocompatible and are capable of retaining considerable amounts of water. This action of water absorption and expulsion mimics closely the physiological function of a NP as a shock absorber. In the biomedical industry, PVA hydrogels have already been used to manufacture contact lenses, lining for artificial hearts, for drug delivery applications and potentially many other future biomedical uses.

The goal of this project is to create an injectable PVA hydrogel system to replace the nucleus pulposus of the intervertebral disc. It has been envisioned that this PVA hydrogel will use a one-cycle heating and cooling protocol for injection. The solid phase PVA hydrogel will be heated till liquid and cooled until reasonable viscosity is achieved before being injected through a cannula into the disc space. The injected liquid PVA hydrogel will conform to the nucleus space, continuing to cure (and solidify) till it reaches its solid phase properties.

This thesis has attempted to characterize and optimize four crucial parameters that will influence the PVA hydrogel's success as an injectable NP replacement implant: Solid phase swelling capacity, modulus of elasticity (stiffness), liquid phase extrusion pressure through a cannula and its curing rate. Customised equipments were designed and manufactured to experimentally measure the mentioned parameters of this PVA hydrogel.

## Chapter 2: Literature Review

#### 2.1 Intervertebral disc

The human spine consists of 24 vertebral bodies, each with an intervertebral disc sandwiching between two adjacent vertebral segments. The combined height of the 23 intervertebral discs in a spinal column accounts for 20–30 % of the human spine [6]. The human spine, interconnected by a complex system of facet joints, ligaments and muscles, can be classified into 3 sections, starting from the top: the cervical, thoracic and lumbar spine.

The cross-sectional areas and heights of the intervertebral discs increase towards the base of the spinal column, where the cervical discs sporting average cross-sectional areas of 305 mm² and the lumbar discs, being the largest, averaging 1,055 mm² [7]. Disc heights are approximately 3-5 mm at the cervical levels and 11–16 mm at the lumbar levels [8-10]. This evolution of increasing cross-sectional areas and heights towards the lumbar discs correspond to the magnitude of load each disc shares respectively. Unsurprisingly, lower lumbar discs are the most susceptible to injuries and degeneration due to the higher loads they carry.

#### 2.1.1 Biochemistry & function of the intervertebral disc

The intervertebral disc is the largest avascular tissue in the human body. It consists of an outer lamellar annulus fibrosus (AF) that encompasses a gel-like inner nucleus pulposus (NP). A cartilaginous endplate lies between each layer of intervertebral disc and vertebral body. In addition to acting as ligaments that allow for motion between adjacent vertebras, the intervertebral discs also allow for axial load transfer, serving as shock absorbers for compressive loads that occur during daily activities.

The NP has a jelly-like consistency comprising 70–90 % water weight while the AF has as 60-70 % water makeup [11]. NP cells have a low average cell density of 3.8 x 10<sup>3</sup> /mm<sup>3</sup>. NP cells synthesize proteoglycans and collagen [6]. Aggrecan is a negatively charged polysaccharide that makes up 90 % of the proteoglycans. Negatively charged polysaccharides have poly-electrolytic properties, leading to osmotic pressures of 0.05-0.25 MPa within the NP [12]. The osmotic pressure gives the NP its turgid properties.

Intervertebral disc pressures significantly vary depending on the loading condition and the posture of the subject. They can vary between 0.1-2.3 MPa [13-15]. The physiologic loads experienced by the spine due to daily activities result in diurnal fluctuations of about 25 % of the disc's fluid, being expelled during daytime and imbibed overnight [16].

The AF essentially is a fibre re-enforced composite, with an average cell density of 9 x  $10^3$  mm<sup>3</sup> [6]. It consists of mostly structured collagen fibrils forming fibrous tissue encasing the NP. The AF dictates the elastic and tension-resisting properties on the intervertebral disc, allowing for a degree of flexion, extension, lateral bending and axial rotation movements [17;18]. The fibrous tissue limits the segmental deformation that occurs during spinal movements. However, it does not bear axial loads as well as the NP does.

The vertebral endplate has an average thickness of 1 mm thick [19], comprising of a bony and a hyaline cartilage portion. Each endplate is sandwiched between an intervertebral disc and a vertebral body. A healthy endplate prevents the NP from bulging into the adjacent vertebral body, as well as contribute to the shock absorption of the spine. The cartilage portion of the endplate acts as a semi-permeable membrane, governing the diffusion pathway of nutrients and wastes to and fro in the intervertebral disc [19].

#### 2.1.2 Degenerative disc disease & lower back pain

About 70 % of the world's population will experience some form of lower back pain at least once in their lifespan [20]. However, this back pain is by no means a clear cut symptom of a deteriorated intervertebral disc. Conversely, persistent back pain is almost always a clinical manifestation of disc degeneration. This is especially true for the lower lumbar discs, where most chronic back pain originates [20]. Lower lumbar discs are the most susceptible to disc degeneration as they carry the highest loads. Although they have evolved to become the largest intervertebral discs throughout the spinal column, they still seem insufficient to sustain heavy loads throughout the lifespan.

To date, initiators that cause disc degeneration are still being heavily debated upon. However, from the cellular level, one of the most agreed on mechanisms that will propel the onset of disc degeneration is due to the compromised nutrient supply to the intervertebral disc [21-23]. The rate of disc degeneration varies among individuals. However, it may be acerbated due to inferior genetic make-up, excessive or adverse biomechanical loadings on the spine, lifestyle conditions and other compromising health factors such as diabetes [24].

Starting as early as the second decade of life [25], the concentration of proteoglycans within the NP drop from an average of 65 % to about 30 % dry weight of nucleus [24;26]. This decline of proteoglycans, likely due to a lower synthesis rate, directly leads to a loss in concentration of other matrix proteins. Consequentially, the NP starts to lose its ability to re-imbibe water and to exert osmotic pressure. This results in a decreased ability to absorb and distribute loads efficiently.

Over time, the disc will become stiffer due to the permanent loss of water content. The properties of this degenerating disc will shift towards a more solid-like behaviour [27;28]. It will start to have creep properties, where its height becomes permanently decreased. Resultantly, the AF will incur increased axial load transfer. Eventually, repetitive load assaults

may give rise to cracks and fissures within the collagen fibrils of the AF [26].

The different stages of disc degeneration have been characterized by Thompson *et al* [29] in a 5-stage scheme, focusing on changes in the intervertebral disc morphology, as shown in Figure 1. A detailed histological assessment on disc degeneration has been done by Boos *et al* [23].

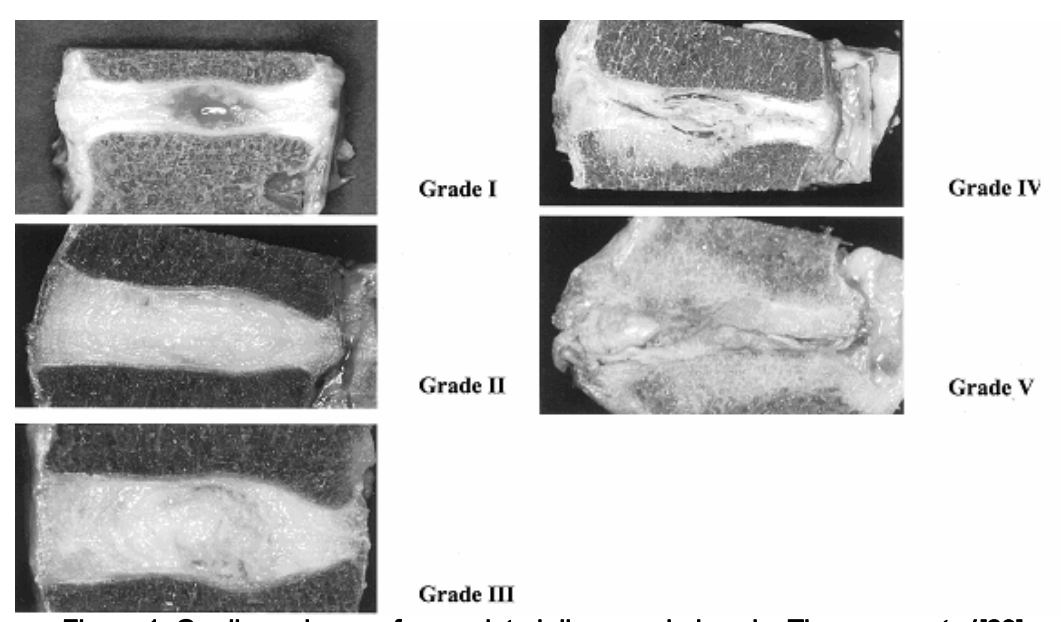


Figure 1: Grading scheme of age-related disc morphology by Thomspon et al [29]

#### 2.2 Current treatments

Current treatments do not reverse the degeneration process of the intervertebral disc (IVD). They only may delay disease progression or stabilize the existing condition of the IVD. The recommended initial treatment for back pain is bed rest, followed by prescriptions of analgesics, anti-inflammatory drugs or muscle relaxants to reduce inflammation and pain. Other conservative treatments such as massage, physical therapy, spinal manipulation and local injection are aimed to reduce inflammation or to strengthen muscles around the spine, or both.

While most of the people can cope and do improve with conservative treatments, those with persistent disabling pain eventually turn to surgical interventions. The United States had over 500,000 spinal surgeries done per year. In 2001, more than half of the spinal surgeries were spinal fusions [30]. The inclination towards surgical intervention has been increasing since the 1980s and seems set to continue. Spinal surgery related technological advances, increased spinal fellowship programs and increased reimbursement to physicians and hospitals are thought to have encouraged this on-going trend [31].

Current treatment modalities are considered to be sub-optimal at combating degenerative disc disease, therefore propelling the research for alternative solutions. Disc arthroplasty, nuclear replacement and biological therapies are the emerging technologies that may one day replace spinal fusion.

#### 2.2.1 Spinal fusion

Literally, spinal fusion surgery fuses two adjacent vertebrae together. The deteriorated intervertebral disc is first removed. An intervertebral device (often a metal or polymer cage) is than inserted to maintain spine alignment and height of the disc space. Bone tissue, usually from the patient, will act as the filler within the intervertebral device, so that bone fusion across the intervertebral space can eventually occur. The bone fusion process usually takes about 6 to 12 months.

Spinal fusion is regarded to be a sub-optimal solution. To date, spinal fusion clinical success rates are low and its long-term benefits are still being questioned [32]. It has an alarming 7 % rate of instrumentation failure and 15 % of the surgeries fail to achieve a solid fusion mass [32]. Among "successful" surgeries, there are only a very limited percentage of people who actually do become free from pain. Recently, Fritzell *et al* [33] published a randomized study with over 2 years of follow-up after spinal

fusion surgery. Results showed that only about 30 % of the patients who underwent spinal fusion became free from pain.

The most problematic long term complication is the cascade of adjacent disc degeneration that radiates from the fusion segment, even after back pain has been relieved [34;35]. A solid fusion is compensated by higher motion and stress at adjacent disc levels, thereby theorized to acerbate the rate of adjacent disc degeneration [36].

Nevertheless, spinal fusion has been the gold standard to surgically treat degeneration for almost 100 years [37]. It continues to be the most common surgical procedure for advanced stages of degenerated intervertebral discs.

#### 2.2.2 Disc arthroplasty

Ideally, an artificial disc should preserve adequate motion of the spinal segment during compression, bending and torsion. An intervertebral disc's unique abilities to transmit, attenuate and distribute stress across its entire cross-sectional area should also be addressed. Finally, during surgery, the positioning of the artificial disc must be taken into account to restore overall disc height, spinal alignment and stability [38].

Presently, there are four modern major disc arthroplasty devices (total disc replacements) either in investigational trials in the United States (US) or have already been approved by the US food and drug administration (FDA). The Charité artificial disc (DePuy Spine Inc.) approved by FDA in October 2004, was implanted over 15,000 times in over 30 countries [39]. The SB Charité III shown in Figure 2a is a biconvex, ultra-high molecular weight polyethylene spacer sandwiched by two Cobalt-Chromium (Co-Cr) alloy endplates coated with titanium and hydroxyapatite coating. Figure 2b shows a ProDisc (Synthes Inc.), also a metal-on-plastic device with Co-Cr endplates and a spherical polyethylene insert which articulates with the opposite base plate. Both the Marverick

(Medtronic Sofamor Danek Inc.) and FlexiCore discs (Stryker Spine) are metal-on-metal devices, with ongoing clinical trials (Figure 2c & d).

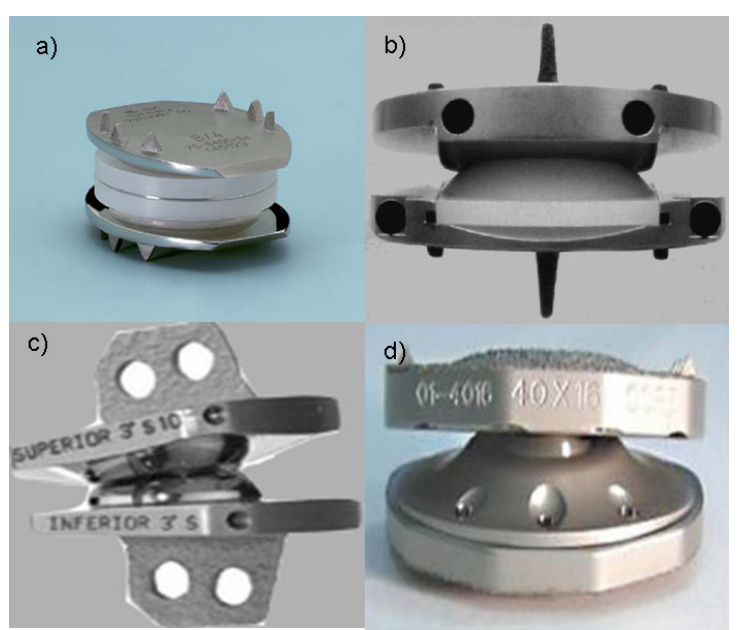


Figure 2: a) SB Charité Artificial disc (DePuy Spine), b) Prodisc (Synthes Inc.), c) Marverick (Medtronic Sofamor Danek Inc), d) FlexiCore (Styker Spine)

Although these devices do help restore the original height of the intervertebral disc segments and confer certain degrees of spinal motion, it is noted that none of them has the ability to undergo axial compression. Indirectly, this translates to a limited ability to attenuate shock and distribute stress. The long term biomechanical performances of these artificial discs are still unknown.

#### 2.3 Nuclear pulposus replacement & future technologies

Nuclear pulposus (NP) replacement aims to restore disc height and re-establish even load distribution without removing the still viable annulus fibrosus (AF). This allows the preservation of the natural biological functions in both the AF and the endplates of an intervertebral disc. Since less of the intervertebral disc's anatomy will be replaced, the complexity

and risk of the surgery is reduced compared to spinal fusion and disc arthroplasty.

NP replacement surgery targets only patients at early stages of disc degeneration, when the AF and endplates are still relatively healthy. Some surgical exclusion criteria has been proposed by Ray [40]. They include: total body weights above 90 kg, back pain deriving from sciatica (nerve pressed upon), a disc height of less than 5 mm, signs of an incompetent annulus, Schmorl's nodes or Spondylolisthesis with grade I or more.

NP replacement treatments can be divided into two main categories: biological therapies and non-biological substitutions. Biological therapies aim to restore function by implanting viable NP cells into the defective intervertebral disc, in order to re-establish NP function. Biological disc therapies are applications in the human tissue engineering domain [41]. Contrary, non-biological substitutions utilize non-biologically active materials to mimic the functions of a healthy NP.

There are currently four biological research approaches to treat disc degeneration: Direct intradiscal injection of an active substance, supplementation of autologous cells, gene therapy to modify gene expression of disc cells and stem cell therapies [42]. Although these areas of research have shown many promising advancements, the realization of a bio-based treatment modality, with the potential to reverse the symptoms of disc degeneration, is still some time away.

Non-biological approaches are already paving their way towards being recognised as an alternative treatment for disc degeneration. Broadly, non-biological NP replacement devices are further characterized as either intradiscal implants or *in-situ* curing polymers. Although none have been approved yet by the US Food and Drug Administration of America (FDA), four NP implants have already been approved for sale in Europe. Lately, an increasing number of companies have decided to develop viable NP replacement devices. Table 1 shows a list of NP replacement devices under different stages of research and development.

Table 1: A summary of non-cell seeded nuclear replacements under investigation.							
Device & Company/Lab	Biomaterial	Stage of research &					
PDN-SOLO® and	Hydrogel (undisclosed)	CE approved <sup>a</sup>	Intradiscal				
PDN-SOLO XL <sup>™</sup> [43]	pellet encased in a		implant				
Raymedica, Inc.	polyethylene jacket	Ongoing U.S. IDE <sup>b</sup> clinical					
raymedica, inc.		trials					
NUBAC™	Polyetheretherketone on	CE approved <sup>a</sup>	Intradiscal				
NODAO	Polyetheretherketone		implant				
		Ongoing U.S IDE <sup>b</sup> clinical					
Pioneer Surgical		trials [44]					
Technology		thalo [11]					
Aquarelle	Semihydrated polyvinyl	Preclinical - Baboon trials	Intradiscal				
	alcohol (PVA) hydrogel	have been completed [45]	implant				
Ctm.dcan Cmina	80% water						
Stryker Spine NeuDisc <sup>™</sup>	2 grades of Modified	Preclinical -	Intradiscal				
INCUDISC	hydrolyzed	Biocompatibility testing	implant				
	polyacrylonitrile polymer	with New Zealand rabbits	implant				
	(Aquacryl) reinforced by	[46]					
Replication Medical	a Dacron mesh						
Inc.	Deliverale and a continue	Olinian Introduction Internal and a	latas dis s al				
Newcleus	Polycarbonate urethane (PCU) elastomer curled	Clinical study, Implanted	Intradiscal implant				
	into a preformed spiral	in 5 patients [43]	impiant				
Zimmer, Spine	into a protormoa opirar						
EBI Regain <sup>™</sup>	Pyrocarbon material	Baboon studies	Intradiscal				
		completed[47]	implant				
Biomet, Inc.		Ongoing U.S. IDE <sup>b</sup> clinical					
Diomot, mo.		trials since 2007 [48]					
Modular intervertebral	Modular intervertebral	Preclinical - In-vitro	Intradiscal				
prosthetic disc (IPD)	prosthetic disc (annulus-	cadaveric calf spine	implant				
D	sparing prosthesis)	models [49]					
Dynamic Spine DASCOR® Disk	Curable nelsurathans	CE approved <sup>a</sup>	In aitu aurina				
Arthroplasty Device	Curable polyurethane and an expandable	o⊏ approveu	In-situ curing polymer				
7 ii ii ii opiaoty Device	polyurethane balloon	Implanted in 16 patients	polymor				
Disc Dynamics Inc.	[50]	Clinical trials in Europe					
SINUX ANR	Curable	CE approved <sup>a</sup>	In-situ curing				
0:::1(D. D. 0	polymethylsiloxane		polymer				
Sinitec/DePuy Spine	polymer without restraining jacket						
Inc. BioDisc	Protein hydrogel	Filed for CE <sup>a</sup> in February	<i>In-situ</i> curing				
DioDioo	1 Totali Hydroger	2007 [51]	polymer				
Cryolife Inc.		L- 1					
NuCore <sup>®</sup> Injectable	Synthetic recombinant	Clinical trials in Europe	In-situ curing				
Nucleus		and United States [43]	polymer				
Cnino Maya Inc	protein hydrogel						
Spine Wave Inc. Gelifex SP and	polymer-based	Preclinical - In-vitro	<i>In-situ</i> curing				
Gelifex IP hydrogels	hydrogels	cadaveric human spine	polymer				
	, 0 50.0	testing [52]					
Synthes, Inc.		that have been approved for					

Blue shaded background represents NP devices that have been approved for sale in Europe. All others are at the preclinical or clinical development stage to our knowledge. Legend: a: CE stands for Conformité Européenne mark, required for European sales of the product. b: IDE stands for Investigational Device Exemption

#### 2.3.1 Intradiscal implants

An intradiscal implant is a solid device which will be placed directly into the intervertebral space. It aims to preserve the viable annulus and endplates, removing only the degenerated nucleus. Therefore, it is a lesser invasive surgical operation compared to that of spinal fusion and disc arthroplasty. However, a substantial surgical window size and annular incision is still required to insert the intradiscal implant into the intervertebral space. An open posterior approach is often needed for its insertion. The intradiscal implant is then carefully placed into the prior created nuclear space and the annulus is re-adapted with sutures.

One of the greatest concerns will be the risk level of intradiscal implant extrusion probability through the annulus wound. Also, care must be taken to select the optimal fitting shape and size of implant to minimize uneven loading across the endplates. Uneven loading has previously resulted in endplate fractures [29]. From the production viewpoint, it will be a challenge to manufacture the required wide range of shapes and sizes of a prosthetic NP replacement device, tailored to each patient's need.

#### 2.3.2 In-situ curing polymer implant

In-situ curing polymer implant is a surgical concept where the polymer is injected into the nuclear cavity while still liquid. The polymer will conform to the shape of the nuclear cavity and cure permanently within. When cured permanently, it is expected to takeover biomechanical loading equivalent to that of a healthy nucleus pulposus and to restore intradiscal height.

One of its most attractive features of an in-situ curing polymer implant is the small annular incision size required for polymer injection, hence reducing the risk of implant extrusion (compared to intradiscal implants). Additionally, an injectable in-situ curing polymer implant eliminates the mentioned challenges posed to manufacturing when

compared with intradiscal implants. Moreover, an in-situ curing polymer implant will allow for a better nuclear cavity fit. Finite element analysis has shown in-situ curing polymer implants can restore normal mechanical behaviour of then annulus fibrosus better compared to intradiscal implants [43].

The In-situ curing polymer implant surgical concept can have important social and economic consequences. Asides being more cost effective due to shorter operating times, patients are expected to recover faster as well as experience less trauma compared to the use of intradiscal implants.

The biggest challenge confronting this design is the selection of a suitable material. In addition to the mentioned biomechanical requirements of an ideal artificial disc under section 2.2.2, this material has to solidify and reach reasonable percentage of mechanical properties within a stipulated time frame. The rate of which the material takes to achieve reasonable mechanical properties is crucial to minimize possible polymer backflow through the annular incision, as well as permanent polymer deformation (if axially loaded at curing phase).

## 2.4 Hydrogels

Hydrogels are a network of polymer chains characterized as a colloidal suspension of liquid in a solid medium. Their unique loose three dimensional network allows for water retention, thus the ability to swell [53].

Hydrogels can be prepared by using monomers, where polymerization is often initiated via radical initiators such as peroxides and azo-compounds. Alternatively, crosslinking existing hydrophilic polymers can also produce in hydrogels. There are two forms of polymer crosslinking, producing either a chemical hydrogel or a physical hydrogel. Once crosslinking occurs, the individual polymer chains are bonded to

adjacent chains and is often transformed into a solid or gel physical state. The extent of crosslinking dictates the molecular mobility within the hydrogel [54].

Chemical hydrogels are formed when crosslinking are achieved via a chemical reaction, where covalent bonding occurs between polymer chains. Crosslinking agents such as electron beams, gamma-irradiation, heat or pressure are often required to create the covalent bonds. Chemical hydrogels are often synthetic.

Physical hydrogels are crosslinked via ionic bonding, hydrogen bonding, van der Waals forces or hydrophobic interactions across segments of polymer chains. Crystallization can occur in physical hydrogels. Physical bonding methods include freeze treatment, partial drying by freezing, cyclic freeze thaw and freezing low temperature crystallization. Natural forming physical hydrogels include collagen, gelatine and polysaccharides.

Depending on the use of hydrogels, they can be classified by their crosslinking method, degree of crystallinity, structural parameters, models for network prediction, swelling behaviour, diffusive characteristics and surface properties. Due to their unique capabilities and versatility, hydrogels are already widely used in the pharmaceutical and biomedical applications [55].

The most common medical application of hydrogels is as a controlled drug delivery system. Often, these hydrogels have a molecular structure that controls the rate of drug diffusion, only releasing its drugs when triggered by specific environmental stimuli, e.g. changes in temperature and pH. Some examples include poly(N-isopropyl acrylamide), poly(acrylic acid), poly(diethylaminoethyl methacrylate). Others such as poly(lactic acid), poly(glycolic acid) and their co-polymers are solely diffusion controlled, where the drug in the hydrogel is released at a consistent rate to its surroundings, as the hydrogel degrades. Other potential and current medical applications of hydrogels include scaffolds

for tissue engineering, contact lens, artificial tendons and artificial skin. An extended list of its uses can be found in Peppas *et al* [5].

Referring to Table 1, the majority of the NP replacement implants are already made from hydrogels. Its established biocompatibility, high mechanical strength, innate swelling ability and elasticity are some of the many desired material properties that have boosted its popularity as a NP substitute.

## 2.4.1 Poly(vinyl alcohol) hydrogel

Poly(vinyl alcohol), PVA, is a synthetic polymer. A fully hydrolyzed PVA consists of repeated monomer blocks of vinyl alcohol groups. Vinyl acetate is polymerized to poly(vinyl acetate), which is hydrolyzed to form PVA (shown in Figure 3). The hydrolysis reaction is not usually complete; thereby PVA polymers often have certain percentage of acetate and hydroxyl groups [56].

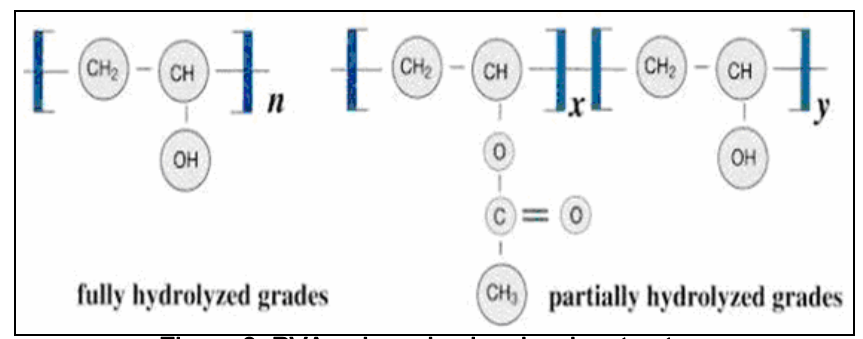


Figure 3: PVA polymerized molecular structure

The degree of hydrolysis is defined as the extent at which hydrolysis occurs within a polymer chain. Commercial grades of PVA polymers are often characterized by the degree of hydrolysis and molecular weight. The degree of polymerization can also be used to characterize PVA. The degree of polymerization is defined by the number of repeat units in an average polymer chain at a specific time during the polymerization reaction. Both the degree of hydrolysis and degree of

polymerization determines PVA's solubility in water, crystallisability, mechanical strength and diffusivity [56].

Although PVA can be crosslinked via chemical means, physical crosslinking can avoid possible toxicity derived from the presence of crosslinking agents. This advantage is especially important if the PVA is to be utilized in a biomedical application. Furthermore, due to the presence of crystallites, physically crosslinked PVA often exhibit higher mechanical strength compared to chemical or irradiative crosslinking methods [56]. The crystallites serve to redistribute mechanical loads across the three-dimensional structure of PVA.

#### 2.5 Hydrogel potential as a NP replacement

Despite being widely used as materials for biomedical applications, hydrogels generally are limited by their weak mechanical properties when used in load-bearing devices. Material research eventually resolved this limitation. Recent research started exploring the application of hydrogel as a NP substitution material [57-61] and other load-bearing scenarios such as for cartilage replacements [62;63]. Table 1 tabulated a non-exhaustive list of NP replacement devices at different stages of research and development. Additionally from Table 1, majority of the companies used hydrogels to develop a feasible NP replacement device.

DASCOR® (Disc Dynamics Inc. Eden Prairie, MN) is an *in-situ* curing polymer implant. It is one of the three hydrogel material NP replacement implants that have been awarded the CE (Conformité Européenne) Mark [64], a requirement for sale within Europe. The other nuclear implants that have been awarded the CE include the PDN (Raymedica Inc. Minneapolis, MN), and NUBAC<sup>TM</sup> (Pioneer Surgical Technology. Marquette, MI). These nuclear implants are intradiscal nuclear implants.

The DASCOR® replacement strategy involves inserting an expandable polyurethane balloon into the nucleus via a catheter after removing the diseased NP. Liquid polyurethane is then injected and contained within the balloon. This allows customised shape conformation of the injected polyurethane implant to occur *in-vivo*. Furthermore, the balloon will retain the liquid polyurethane within, minimizing leakage probabilities out of the nucleus space.

Raymedica Inc's Prosthetic Disc Nucleus (PDN) is the most extensively researched intradiscal implant, with research work spanning over 5 years. By 2002, 423 patients in Europe and Africa were already implanted with a 90 % success rate [65]. It is made of an undisclosed hydrogel encased in a polyethylene jacket.

NUBAC<sup>TM</sup> is a polyetheretherketone on polyetheretherketone intradiscal implant developed by Pioneer Surgical Technology (Marquette, MI). Load sharing and uniform stress distribution under various physiological loading conditions is expected to be achieved through the ball and socket design. It has been CE approved and has begun its Investigational Device Exemption (IDE) study at the Marquette General Hospital in Marquette, Michigan, United States.

#### 2.5.1 PVA hydrogel as a NP replacement

Bao and Higham filed several US patents for using PVA hydrogels as an intradiscal NP replacement implant [66-69]. They have developed various PVA based NP replacement devices, with a water content ranging from 30 to 90 weight percentage (wt%) and with unconfined compressive strength modulus of about 1 to 4 MPa. They were the first to introduce a PVA hydrogel that had sufficient mechanical and swelling properties [70].

Stammen *et al* [71] characterized 2 formulations of PVA hydrogels, with approximately 75 wt% and 80 wt% respectively. They were found to have a compressive strength modulus of about 1–3 MPa, in the strain interval of 0.1-0.3. These hydrogels have been proposed for medical

applications such as replacing the articular cartilage, disc implants and other load bearing bio-applications.

The Aquarelle (Stryker Spine, Allendale, NJ), an intradiscal implant, uses a freeze-thaw technique to make a physically cross-linked PVA hydrogel with water content of about 80 wt% and has a biomechanical durability up to 40 million cycles [43]. The Aquarelle was used in a 24 months survival baboon study; Allen *et al* [72] reported about one quarter of the test cohorts experienced implant extrusions.

Thomas *et al* [73] varied proportions of PVA and PVP, poly(vinyl pyrrolidone), concluding that a crosslinked network prepared with 99 % PVA (143K) and 1 % PVP (40K) resulted in the highest network stability, This is also proven true when compared to 100 % pure PVA samples. Subsequently, the above PVA/PVP blend under went further experimentation including unconfined and confined compression tests, unconfined fatigue tests and biomechanical fatigue characterization while inserted in human cadavers [52]. Gelifex Inc. was formed in 2002 to further develop the associated family hydrogels as a nucleus replacement device. Gelifex has since been acquired by Synthes Inc. (West Chester, PA) in 2004. A US patent has been issued for the above formulation [74].

#### 2.6 Novel PVA hydrogel as an *in-situ* curing NP replacement candidate

An injectable *in-situ* curing NP replacement material is envisioned to be performed, as shown in Figure 4. The hydrogel is stored at room temperature and sealed in a portable container indefinitely. A small surgical incision will be made through the annulus to reach the NP. The degenerated nucleus pulposus will be surgically removed using rangeurs and shavers. When the nucleus cavity is ready for injection, the hydrogel is heated to 100 °C till it becomes liquid. It will then be cooled down to an injection temperature, low enough not to cause burns and at a viscosity that is still injectable through a suitable cannula. A handheld injection

applicator is envisioned to inject the hydrogel into the nuclear space. The hydrogel is then left to cure within the nucleus cavity.

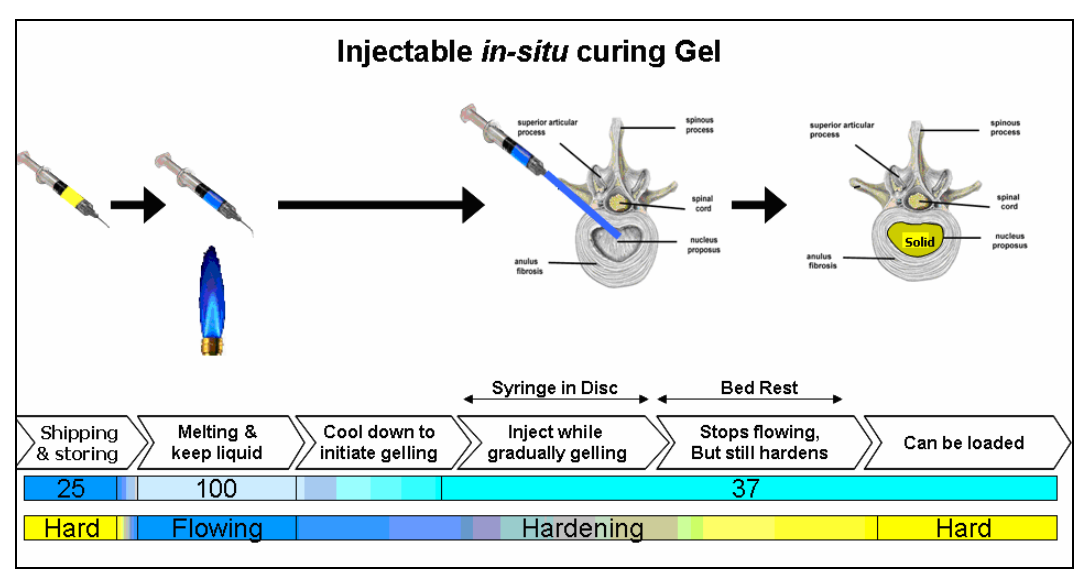


Figure 4: A breakdown schematic diagram of an injectable hydrogel NP process

A proprietary PVA hydrogel (InnoSpine Inc. AG, Schlieren, Switzerland) presently is being evaluated at the Orthopaedic Research Laboratory. The goal is to optimise their hydrogel, to be used as the injectable NP replacement material. The research collaboration was initially helpful to characterize basic material properties of different PVA formulations. The data were used to continuously improve the formulation for its application as a NP replacement. After several rounds of screening, two PVA hydrogel formulations were finally tested in a comprehensive manner and completed.

The patented PVA hydrogel utilizes its thermoplastic properties to produce a melt that can be casted into moulds for curing into solid blocks. Compared to conventional PVA synthesis methods, this novel system allows crystallization to take place at higher temperatures, hence bypassing the need for conventional repetitive freeze-thaw cycles. Additionally, its unique thermoplastic properties enables it to undergo cycles of melting and solidifying within a closed system, seemingly without alterations of its mechanical and chemical properties. Therefore, this PVA

hydrogel formulation has a potential to become a suitable injectable *in-situ* cured nucleus replacement candidate.

Given the proposed use of this PVA hydrogel and the proposed surgical procedure, several research questions need to be answered. Swelling capability, stiffness, required extrusion force and hydrogel curing rate are identified as crucial. The thesis' author has conducted, in preparation of the thesis topic, several screening tests using initial PVA formulations. Rationales regarding the mentioned parameters, selected screening results and discussion is summarized.

#### 2.6.1 Swelling

It is essential that the PVA hydrogel has an intrinsic ability to imbibe water and expand. This ability mimics the osmotic behaviour of a nucleus pulposus. Screening results were plotted accordingly to compare hydrogels with different water contents, sizes and lapsed time after production. Graphs shown in Figure 6 to Figure 8 suggest that the hydrogel's swelling rate and equilibrium volume are dependent on various parameters. Therefore, further examination of its swelling properties will be crucial to conclude its suitability as a nucleus replacement candidate.

From Figure 5, most hydrogels reach a swelling equilibrium weight at about 50 hours. After which, the hydrogels showed weight loss when soaked in the phosphate buffer saline (PBS) for prolonged periods of time. The weight loss is believed to be due to leaching, where unreacted monomers diffused out of the polymer networks into the surrounding fluid. Another possibility is dissolution.

Mallapragada and Peppas [74] had tried to characterize the dissolution mechanism of semi-crystalline PVA in water. As the name suggests, dissolution is a process where the polymer dissolves into the solution. They have proposed that the crystalline structure of PVA unfolds itself layer by layer in the presence of a solvent, joins the amorphous regions of the polymer before eventually untangling and dissolving.

Thomas *et al* [73] also documented loss of PVA/PVP polymer dry mass after swelling for prolonged periods in deionised water. Dissolution was attributed as the main cause of mass loss.

Results from Figure 6 indicate that different initial specimen sizes of the hydrogels showed to different equilibrium swelling weight percentages. Figure 7 suggests that the swelling ability of hydrogels is dependent on its storage duration, from the date of manufacture. Its swelling ability seemed to decrease as the lapsed time after manufacture increased. It is non-conclusive if the hydrogel's swelling ability stabilises overtime.

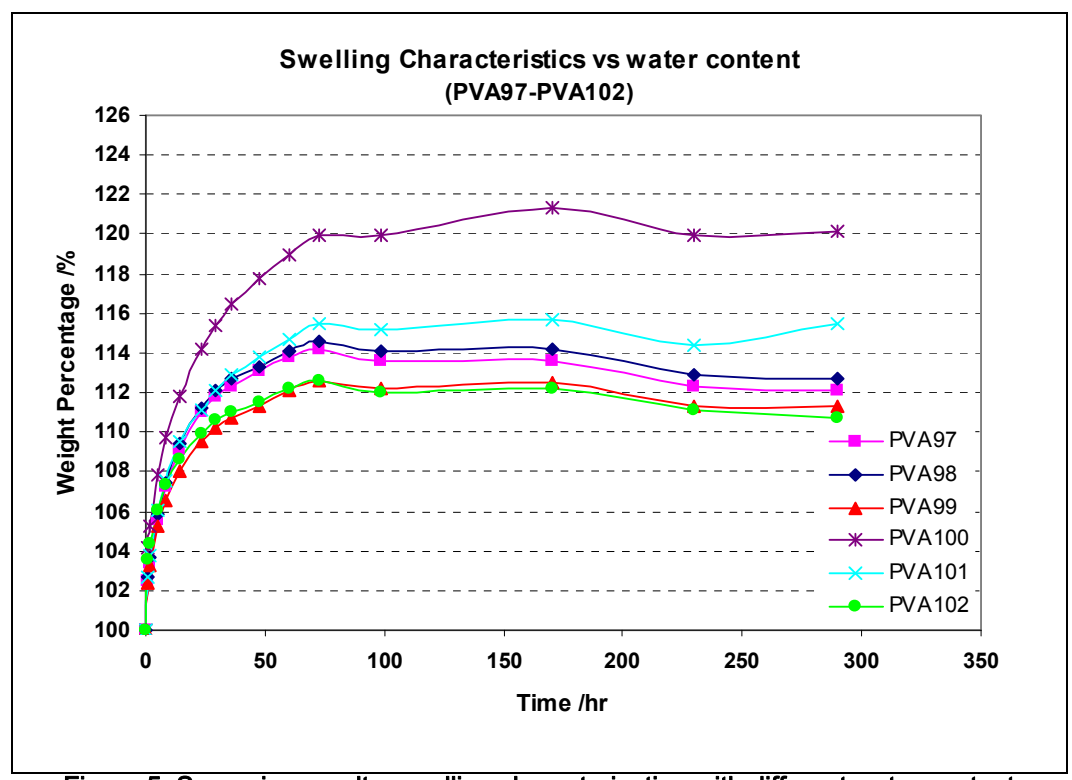


Figure 5: Screening results, swelling characterization with different water content percentage

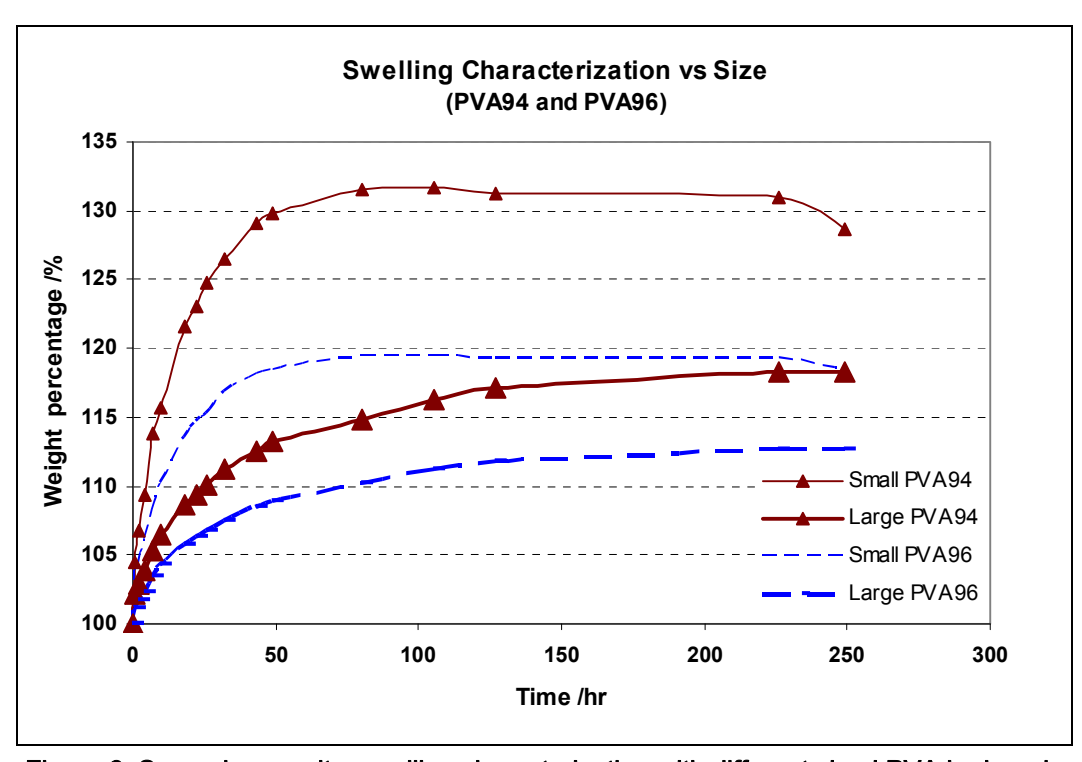


Figure 6: Screening results, swelling characterization with different sized PVA hydrogels

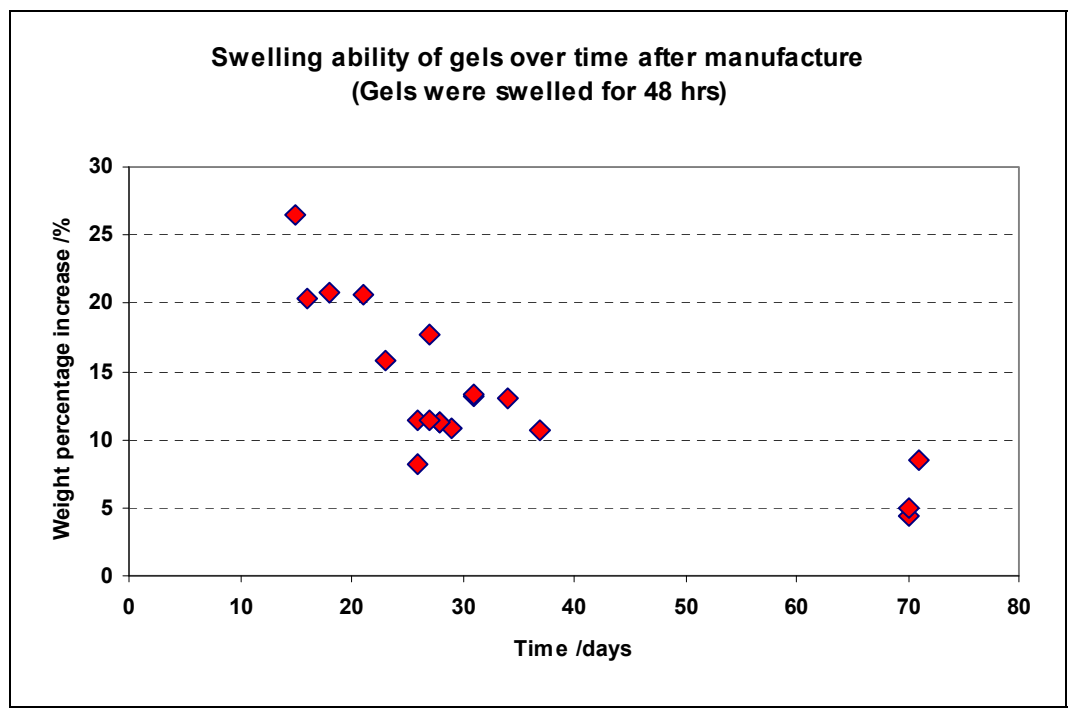


Figure 7: Swelling characterization vs. lapsed time after production

#### 2.6.2 Stiffness

The PVA hydrogel should have the modulus of elasticity comparable to that of the native NP. 10 to 30 % height loss of an intervertebral disc is reported to be normal diurnal variations [75;76]. Wilke et al measured in-vivo nucleus pulposus axial pressures of a human volunteer's non-degenerated L4-L5 intervertebral disc. Resulting pressures ranged from 0.1 MPa to 2.5 MPa [77], dependent on the subject's body positions and type of activity. Sato et al measured intradiscal pressures from eight volunteers at the L4-L5 disc levels, reporting an average of 1–2 MPa based on standing and sitting positions [78].

If the PVA hydrogel is too stiff, similar to the effect of Polymethyl methacrylate (PMMA) cement used for vertebroplasty, it could result in fractures of adjacent vertebral endplates during normal spinal motion [79]. Conversely, a too low stiffness would not transmit the normal proportion of axial load, causing the annulus fibrosus to bear a higher portion of loads than normal. Overtime, this may lead to an accelerated degeneration of the intervertebral disc.

#### 2.6.3 Extrusion forces

Designing a hand held pressure applicator to inject the hydrogel requires the knowledge of feasible pressure magnitudes to be encountered. A typical hand-held pressure applicator should exert about 10 MPa, after which the economics of scale and mechanical feasibility outweighs its usefulness. Additionally, the hydrogel should operate within an acceptable time frame to be useful. Exceeding the operational window would only prolong the surgical procedure without adding safety or convenience. Therefore, it is essential to determine an optimal operational pressure and hydrogel injection time.

#### 2.6.4 Curing properties

After the hydrogel has been injected into the intervertebral space, it is necessary to advice the patient of a minimum required bed rest time and, or spine immobilization period. Ideally, the hydrogel should reach a 100 % of its fully cured stiffness state and its other material properties immediately after surgery. Hence, the rate of which the hydrogel gains its fully cured properties will be important to the success of any NP replacement.

### 2.7 Long term studies

Creep and fatigue properties of the hydrogel are equally pivotal factors which will eventually determine its success as a NP replacement material. These material properties were not thoroughly characterized. Nevertheless, estimates can be derived from screening results.

#### 2.7.1 Creep and fatigue

#### **Experimental procedure**

The hydrogel specimen was pre-soaked in PBS at 37 °C for 48 hrs (1:1 height to diameter ratio, refer to Chapter 3 for hydrogel preparation). The hydrogel specimen (sample size n = 1) was then subjected to an unconfined compressive load of 0.7 MPa, for 12 hrs in PBS at 37 °C. The MTS (Mechanical testing system) machine was load-controlled and its load, displacement, time were duly recorded (Specifications detailed in Chapter 3). After 12 hrs, the static load was removed and the hydrogel specimen's height was intermittently monitored using a digital vernier caliper.

The objective was to screen the different PVA hydrogels' creep and plasticity behaviour and not to fully characterize it. Seven different PVA hydrogel formulations were tested.

#### Results and discussion

Figure 8 shows an example of a resultant graph. The height after 48 hrs swelling was defined as 100 %. The graph allowed readout of the following parameters: 'a' indicates the initial height loss due to its elasticity, 'b' is the height loss due to creep properties of the hydrogel, 'c' is its instantaneous recovery after released of the 0.7 MPa load and 'd' shows its long-term height recovery, being indicative for its plasticity.

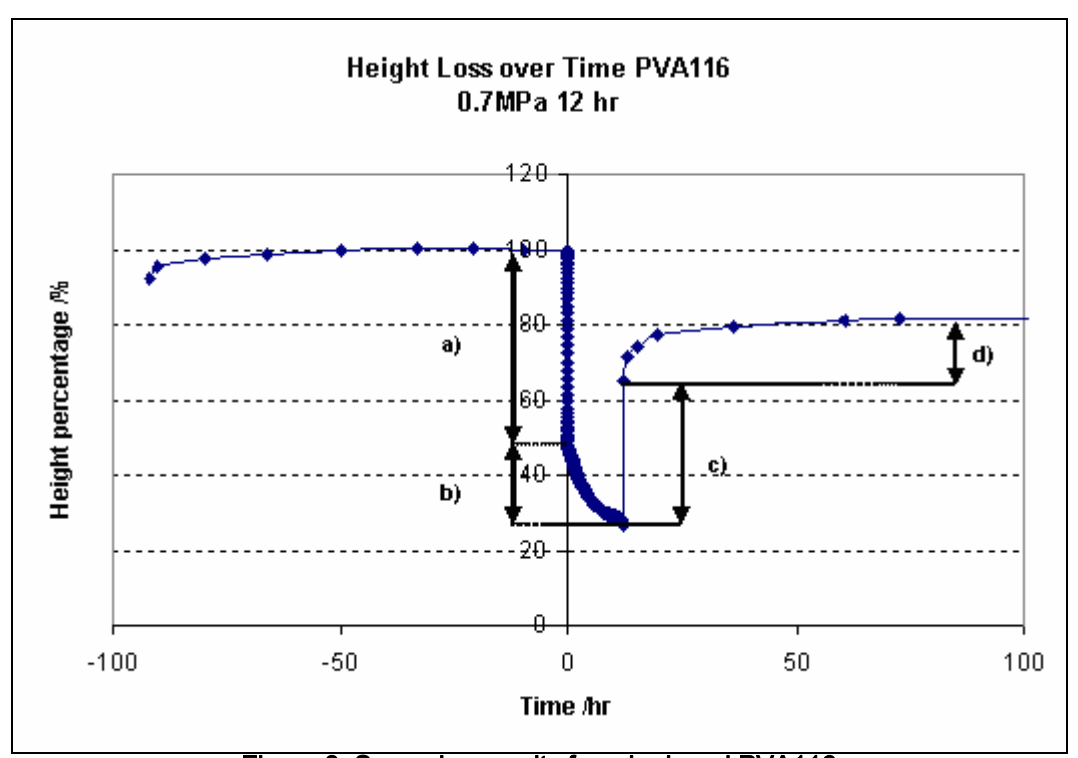


Figure 8: Screening results from hydrogel PVA116
Legend: a) Initial height loss due to its elasticity, b) Height loss due to creep,
c) Instantaneous recovery after load released d) Plasticity

Table 2 tabulated normalized ratios to the hydrogels' swollen height. A/(A+B) characterizes the elasticity of the material, C/A characterizes its elastic recovery ability, (A+B)/(initial height) characterizes the percentage height loss after 12 hrs of static load. (C+D)/(Initial height) characterizes the percentage height recovery after 12 hrs.

Results from Table 2 suggest that the materials were elastic and had an average permanent deformation of about 20 % after 12 hrs static

loading and an extended recovery period. The deformation range was higher than desired. A higher elasticity material will be more favourable. It should be noted that it is hard to translate the resultant creep property to a confined annulus setting. The hydrogel is unable to expend laterally in a confined annulus setting; hence its height loss may be reduced with similar static loading conditions.

Table 2: Screening results of creep experimentation

	PVA104	PVA106	PVA108	PVA110	PVA112	PVA114	PVA116
Initial height loss, A	0.49	0.56	0.44	0.45	0.53	0.57	0.51
Height loss due to creep, B	0.19	0.37	0.22	0.18	0.33	0.19	0.22
Remaining height left on MTS	0.33	0.07	0.33	0.37	0.14	0.24	0.27
Instantaneous recovery, C	0.29	0.44	0.35	0.19	0.46	0.37	0.34
Long term recovery, D	0.15	0.20	0.17	0.20	0.18	0.18	0.16
Permanent deformation	0.23	0.29	0.15	0.24	0.22	0.20	0.23
A/(A+B)	0.72	0.60	0.66	0.72	0.61	0.75	0.70
C/A	0.59	0.78	0.80	0.41	0.87	0.65	0.68
(C+D)/Initial height	0.44	0.64	0.52	0.39	0.64	0.56	0.50
(A+B)/initial height	0.67	0.93	0.67	0.63	0.86	0.76	0.73

Creep and fatigue characterization require much more resources to be tested and are time consuming to be performed. Therefore, complete characterization is postponed until the hydrogel formulations are further optimized.

# Chapter 3: Selected Research Approach

The selected hydrogel should have functional properties similar to the ones of a healthy nucleus confined in an annulus. Due to difficulties in separating the load bearing ability between the nucleus and the annulus fibrosus, based on current literature, a value of about 2 MPa E-modulus was chosen as an ideal value. This material based stiffness value is chosen to balance hydrostatic and direct load bearing properties of the nucleus, as well as to mimic overall intervertebral disc stiffness. Screening data showed up to 25 wt% swelling of the hydrogel. To test the hydrogel's apparent stiffness change for different water contents, the hydrogel's free swelling properties were characterized; stiffness was measured for different swelling intervals.

The hydrogel was to be optimized for injection at the highest possible viscosity and cured *in-vivo* within the shortest possible time frame. While mimicking injection conditions typical for a clinical setting, different hydrogel injection temperatures and waiting periods before injection were tested.

The hydrogel, after melting and injecting, will eventually regain final stiffness over time. Establishing the injected hydrogel's rate of stiffening is essential to recommend a patient of an appropriate back immobilization time duration, before normal load bearing can commence.

Specific research aims, as listed in section 3.1 below, were defined.

#### 3.1 Research aims

The 4 essential parameters selected for thorough characterization. Experiments were designed to study each parameter.

1) Swelling volume as a function of time while submerged in PBS at 37 °C, simulating physiologic conditions.

- Stiffness and strength were determined from unconfined compression. Strain dependent stiffness comparisons before and after eight weeks submersion in PBS.
- 3) Extrusion pressures for injecting the liquid hydrogel through a typical sized cannula. The extrusion pressures were related to the PVA hydrogel formulations, environmental temperatures and lapsed time before injections.
- 4) The stiffness over time after re-melting PVA hydrogels was measured for three different set temperatures.

## Chapter 4: Material & Methods

## 4.1 PVA hydrogels

2 different formulations of poly(vinylalcohol), PVA, hydrogels were tested. All hydrogels samples were provided by InnoSpine Inc. (AG, Schlieren, Switzerland). Each glass tube was filled with hydrogels to about three quarters full (11.9 mm inner diameter and 100 mm height) and was individually sealed to prevent water vapour loss to surroundings. Both PVA121 and PVA14X were physically crosslinked, and had the exact same mixture of PVA macromolecules, with the same distribution of molecular weight.

The first set of PVA hydrogels, PVA121, was fully hydrolyzed and consisted of 65.8 wt% of water. PVA121 was manufactured in 4 batches that used identical process conditions. Each manufactured batch of PVA121 had nine tubes and was differentiated by numbers from batches #1 to #4.

The second set of PVA hydrogels arrived about one and a half months later. Similarly, PVA14X came in 4 batches. PVA141 (batch #1) and PVA143 (batch #3) had 9 tubes, PVA142 (batch #2) and PVA144 (batch #4) had 8 tubes. PVA14X series were also fully hydrolyzed, with 49.4 wt% water. To introduce radiopacity, 17 wt% Barium Sulphate was incorporated in the formulation. Assuming that the Barium Sulphate is fully inert during the gelling process, the gel phase had 59.5 wt% of water.

# 4.2 Swelling capability

Screening results (Refer to section 2.6.1) discussed various parameters that can affect the hydrogels' swelling ability. The possible swelling variables include initial water percentage of the hydrogels,

volume and shape of the hydrogels subjected to swelling, as well as age of the hydrogels.

In response to the screening results, possible variables were eliminated as much as possible to solely document the swelling properties of PVA121 and PVA14X. Six identical sized specimen from PVA121 and PVA14X, stored for 14 days after manufacture date, were subjected to unconfined swelling in simulated physiologic conditions (submerged in PBS at 37 °C) respectively. Each specimen's weight relative to its initial weight, over a period of eight weeks was recorded and plotted. The swelling experiments were started simultaneously for all 6 specimen of PVA121, as well as that of PVA14X, to minimize result variability.

## 4.2.1 Experimental procedure

## **Hydrogel extraction & slicing method**

To extract the casted hydrogel rod from its glass tube, the glass tube was wrapped between towels, placed longitudinally into a vice and compressed till the glass tube cracked. The hydrogel rod (~70 mm length) was then very briefly washed under running water to remove remaining shards of glass. One end of the hydrogel rod had a conformed rounded end shape of the glass test tube, while the other surface is usually uneven.

Due to the soft texture of the hydrogel, it was impossible to accurately slice them with a knife, to achieve a 1:1 height to diameter ratio cylindrical specimen with right angled, flat and parallel surfaces. Therefore, referring to Figure 9, a slicing platform with a fixed blade and an adjustable height stand was constructed. The hydrogel rod was inserted into the socket of the milling machine. The slicing platform had a height stand fixed at 11.9 mm and was clamped with a vice attached to a milling table. The dial indicators of its x, y and z-axis feed was adjusted accordingly, until the protruding base of the hydrogel rod barely rested on the height stand of the slicing platform. When the milling machine ran, the

hydrogel rod rotated axially. The vice, with the attached slicing platform, was manually adjusted along the x & y axis to slice the hydrogel specimen to feature flat and parallel surfaces with the 11.9 mm height.

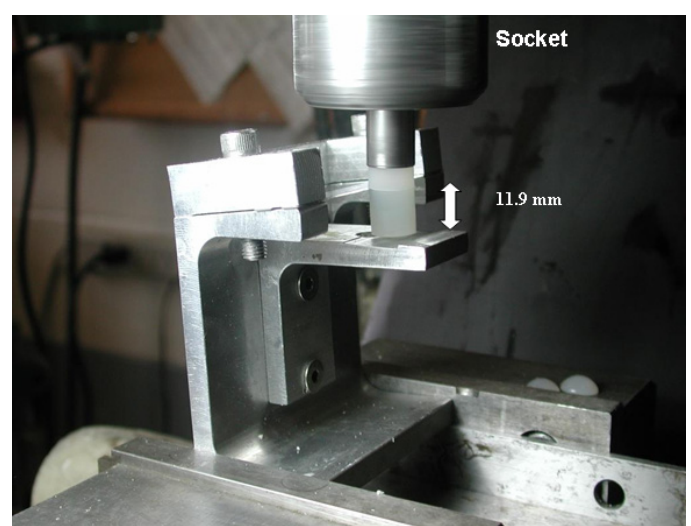


Figure 9: Slicing setup to cut hydrogel rods into 1:1 height to diameter ratio

## Phosphate buffer saline (PBS) preparation

10x stock solution of PBS was prepared by dissolving 80.0 g sodium chloride (NaCl), 2.0 g potassium chloride (KCl), 14.4 g disodium hydrogen phosphate (Na<sub>2</sub>HPO<sub>4</sub>) and 2.4 g monopotassium phosphate (KH<sub>2</sub>PO<sub>4</sub>) in 800 mL of distilled water, and topping up to 1 L. The stock solution was then diluted 10 fold with distilled water when ever needed. The pH of the stock solution was about 6.8; when diluted to 1x PBS, its pH was about 7.4.

#### Measurement procedure

The initial weight of each hydrogel specimen was recorded. Each specimen was then submerged in 35 mL of phosphate buffer saline (PBS) at 37 °C and of a pH 7.4. These solutions were tightly capped in 50 mL Fisherbrand polypropylene centrifuge tubes and stored in a 37 °C incubator. Periodically, forceps were used to gently extract the specimen from the PBS. Next, the extracted specimen was dried gently with Kimwipes®, weighed using an analytical weighting balance (Resolution of

± 0.0001g) and returned to their respective containers. The time of weighing and their weights were recorded.

## Data analysis

The weight percentage of the hydrogel specimen was calculated as follows:

Weight percentage [%] = 
$$\frac{\text{Weight at x hrs [g]}}{\text{Initial weight at 0 hrs [g]}} \times 100$$
 **Equation 1**

The weight percentages of the hydrogel specimen were plotted against time to characterize their swelling capabilities.

## 4.3 Unconfined Compression

To characterize any changes in the stiffness of PVA121 and PVA14X over time when exposed to simulated physiologic conditions, its test specimen were subjected to unconfined compression tests before and after specific time intervals immersed in PBS, The MTS (Mechanical testing system) was used to record data for calculating the respective Young's modulus.

#### 4.3.1 Experimental procedure

#### Specimen preparation

All PVA121 specimen were prepared from batch #3. PVA14X specimen utilized hydrogels from PVA141 (batch #1) and PVA143 (batch #3). 3 specimen each of PVA14X were prepared from batches #1 and #3. This measure minimizes potential variation in results due to the differences between batches #1 and #3 for PVA14X.

All specimen had 1:1 height to diameter ratio. For each hydrogel type, three sets of 6 specimen each were pre-conditioned by soaking in 35 mL PBS at 37  $^{\circ}$ C for 48 hrs, 4 wks and 8 wks respectively. The fourth set

of specimens served as the control. The control set was subjected to unconfined compression immediately (0 hrs) after being sliced to the 1:1 dimensions.

#### **Mechanical Testing**

MTS 858 Mini Bionix (MTS Systems Co., Eden Prairie, Minnesoata, USA) was used throughout this project. The important two components of MTS are the actuator arm and the load cell. The MTS Testware-SX version 4.0B software served as the user interface, where inputs and output parameters were set.

Two flat surfaces parallel to each other and perpendicular to the direction of displacement were used to perform the unconfined compression tests. One surface was attached to the actuator arm of the MTS and the other to the opposite side, the load cell. Each flat surface had a thin layer of sandpaper glued on to ensure a better grip of the test specimen.

Forceps were used to remove the hydrogel specimen from the PBS. The hydrogel specimen was gently dried with paper wipes (Kimwipes®) and each specimen's initial height and diameter was measured with a digital vernier calliper trice and averaged. 1 % strain per second till 70 % maximum strain were calculated and entered into the test protocol running on the MTS (Testware-SX version 4.0B). The desired velocity and the final displacement value were translated to the actuator arm. The MTS recorded time, force and displacement at 20 Hz sampling frequency.

The force reading on the MTS load cell was reset to 0 N. The test specimen was then placed on the testing platform. The top surface (attached to the actuator arm) was manually lowered towards the specimen slowly till the force was reading negative. The top surface was then again slowly moved up till the force reading was back at 0 N. This position corresponded to the initial height of the specimen. The unconfined compression testing program was initiated.

## Data analysis

The Young Modulus E, of a material can be derived via the relationship:

$$E = \frac{Stress}{Strain} = \frac{\sigma}{\varepsilon} = \frac{F/A_o}{\Delta l/l_o}$$
 Equation 2

Where

*E* , is the young modulus of a material

F, is the force applied on a material

 $A_a$ , is the cross-sectional area in contact with the force of a material

 $l_a$ , is the original length of a material

*l*, is the current length of a material

Stress,  $\sigma$ , is a measure of force per unit cross-sectional area. Strain,  $\epsilon$ , is the quantified expression of a deformation on a physical body under the action of applied forces. Hence, the Young's Modulus E is a measure of stiffness of the material – commonly termed modulus.

Using the above relationship, stress-strain graphs were plotted. The slope of each fitted straight line was calculated for 5 % strain intervals from 5 to 70 % strain, e.g. 5-10 %, 10-15 %, 15-20 %, 20-25 % etc. These slopes were assumed to be approximately equal to the tangent compressive modulus at strain values of 7.25 %, 12.5 %, 17.5 % etc. Average tangent compressive moduli were then plotted for each specimen and time interval against corresponding strain values.

#### 4.4 Hydrogel extrusion

The hydrogel extrusion setup was designed to characterize the extrusion pressures of hydrogels PVA121 and PVA14X through a typical sized cannula for different environmental temperatures and curing time intervals. A schematic diagram of the custom experimental setup is shown in Figure 10.

## 4.4.1 Experimental setup

## Specimen selection & preparation

Table 3: Classification of hydrogels used for the extrusion experiments

Gel Type	Number of tubes tested, X	Temperature [°C]	Sets of extrusion time points*, y [min]	Test number
PVA121	6	25	-5, 0, 2, 4	1
PVA121	6	37	-5, 0, 5, 10, 20	1
PVA121	6	50	-5, 0, 15, 30, 45, 60	1
PVA14X	3	37	-5, 0	1
PVA14X	3	50	-5, 0, 2.5, 5, 7.5, 10	1
PVA14X	3	60	-5, 0, 5, 15, 30, 40	1
PVA14X	3	50	-5, 0, 2.5, 5, 7.5, 10	2
PVA14X	3	60	-5, 0, 5, 15, 30, 40	2

<sup>\*</sup>Refer to Figure 14 for an illustration of time point vs. real time

A total of 18 test tubes of hydrogel PVA121 and 15 test tubes of hydrogel PVA14X were tested. Table 3 summarized the gel type, the total number of hydrogel tubes tested, the steady-state temperature of the experimental setup and its corresponding set of extrusion time points. The test number specifies the group of which experiments were performed. All experiments executed in test 1 and test 2 was completed within a week's time. The two test groups were spaced apart 4 weeks. Therefore, the two groups have a different storage time lapsed at the time of testing.

#### **Experimental Setup**

The main equipment consisted of a heat-exchanger unit, a pump, a syringe setup and an aluminium testing platform, shown in Figure 10.

The heat exchanger unit had a water reservoir serving as the heat source. Copper coils acted as a heat transfer medium where heat from the water reservoir was transferred into the water circulating through in the copper tubing. The temperature of the water reservoir is adjustable with a dial to the set temperature. 3.4 m length of copper tubing with an inner diameter of 6.35 mm (0.25") and a wall thickness of 0.81 mm (0.032")

were coiled up and placed in the heat reservoir to serve as a heat exchanger unit.

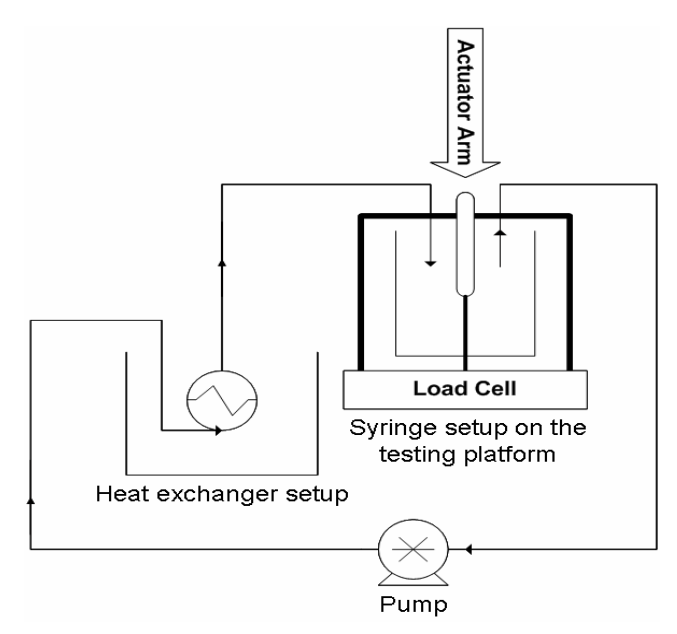


Figure 10: Schematic diagram of the experimental setup used for hydrogel extrusion

The pump motor (Cole Parmer variable speed 7567-70) drove a pump head (Cole Parmer L/S® standard K-07017-20). Silicon tubing (Masterflex C-FLEX, L/S 17, EG-06424-17) connected the setup together. The pump ran at 100 rpm, translating to 280 mL/min of fluid exchange. The silicon tubing was the transport medium, connecting the heat exchanger unit to the testing platform.



Figure 11: Extrusion syringe with the detachable plunger (Including plunger stem)

The syringe setup is featured in Figure 11. The syringe setup had an aluminium syringe body of 125 mm in length, a wall thickness of 3.175 mm (1/8") and an inner diameter of 11.7 mm. The total length from the ball valve to the tip of the cannula was 145 mm. To ensure a uniform inner diameter (ID) within the ball valve, 2 small Delrin® pieces were machined and inserted into the inner walls of the ball valve, ensuring a consistent 8-guage ID of the cannula throughout. The plunger system was comprised of a detachable Delrin® plunger piece and a stainless steel plunger stem. The plunger piece had a female threaded end which complemented the plunger stem male threaded end. The plunger stem was made from stainless steel 316L.

The aluminium testing platform supported an acrylic tank waterbath and the syringe setup. The acrylic tank had a height of 230 mm and held a total volume of about 1.6 L water. A hole was drilled at the bottom of the acrylic tank waterbath and was fitted with a modified brass compression tube fitting. The brass compression tube fitting was designed to allow the cannula end of the syringe to protrude out of the waterbath. This feature ensures extrusion of the hydrogel occurred outside the waterbath. When the waterbath was filled with water and without the syringe, a stopper was used to prevent water leakage from the base of the acrylic tank.

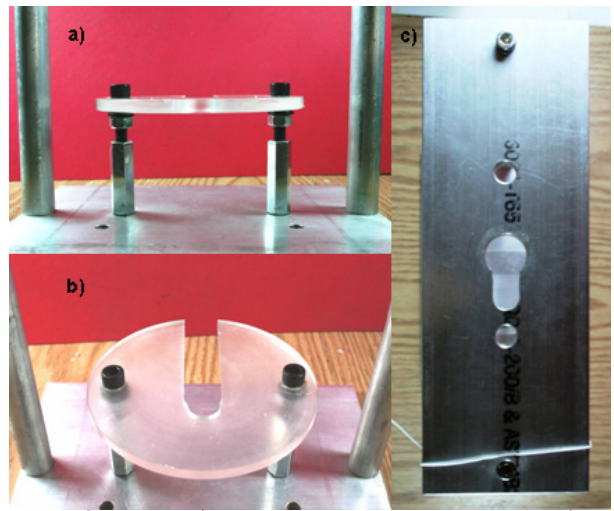


Figure 12: The setup features a) height adjustable disc plate, b) slotted disc plate, c) key-shaped hole on the aluminium stand

Figure 12 shows three distinct features of the aluminium platform, necessary for the operation of this experiment. Figure 12a shows a height adjustable feature on the slotted base plate. Figure 12b shows the slotted base plate which supports the load of the water-filled acrylic waterbath. The slot is required so that the acrylic tank can balance on the plate without hindrance from the protruding modified brass compression tube fitting. Additionally, the slot facilitates the movement of acrylic tank when required (See section 3.4.2 Experimental Procedure below). Figure 12c shows the aluminium stand, featuring 2 drilled holes, allowing the silicon tubing to fit through snugly. The central key-shaped hole was made to enable the ball valve handle of the syringe to pass through as one entity. The tang on the syringe body rests on the aluminium stand during testing.

## 4.4.2 Experimental procedure

Before testing, the water flow temperature in the reservoir was fine-tuned to account for the heat loss within experimental system to its surroundings. A thermometer was used periodically to ensure that the desired temperature was maintained in the acrylic tank waterbath throughout the experiment. The slotted base plate on the aluminium platform was lowered using the screw and nut system. The acrylic tank waterbath was removed so that its modified brass fitting was off alignment from the key shaped hole of the aluminium setup. When the syringe setup was inserted through the key-shaped hole, the entire syringe body remained outside of the acrylic tank. Although the acrylic tank was removed, the heat exchanger setup was unaffected.

Hydrogel rods were extracted from its respective test tubes, washed and dried. Leaving the ball valve of the syringe open, the hydrogel rod with the rounded end was pushed into the aluminium syringe. When

the bulk of the hydrogel rod was inside the syringe, using the tangs of the syringe as a guide, a blade was used to slice off the uneven end of the hydrogel rod, creating a flat surface. Next, the plunger system was used to insert the entire hydrogel rod till it touched the orifice of the syringe. A vacuum pump was then attached to the cannula end. 10 seconds of suction was applied to remove any remaining air between the ball valve and the rounded end of the hydrogel. The ball valve was then closed before the suction was turned off. Subsequently, the male-end plunger stem was removed, leaving the Delrin® plunger piece within.

Input values of velocity and maximum displacement values for the MTS program were calculated. The relationship between volume and height of the hydrogel rod is:

$$Vol = \frac{\pi D^2 h}{4}$$
 Equation 3

Vol is the volume of the syringe body

**D** is the inner diameter of the syringe

**h** is the height of syringe body, where the plunger piece rests

Each extrusion test was standardized to run for exactly 8 seconds. Therefore, the velocity (rate of displacement) was calculated by dividing the length of the hydrogel rod in the syringe over the 8 seconds time interval. Two different volume rates used for extrusion and their respective displacement values rates are shown in Table 4.

Table 4: Relationship between volume, displacement and rate of displacement

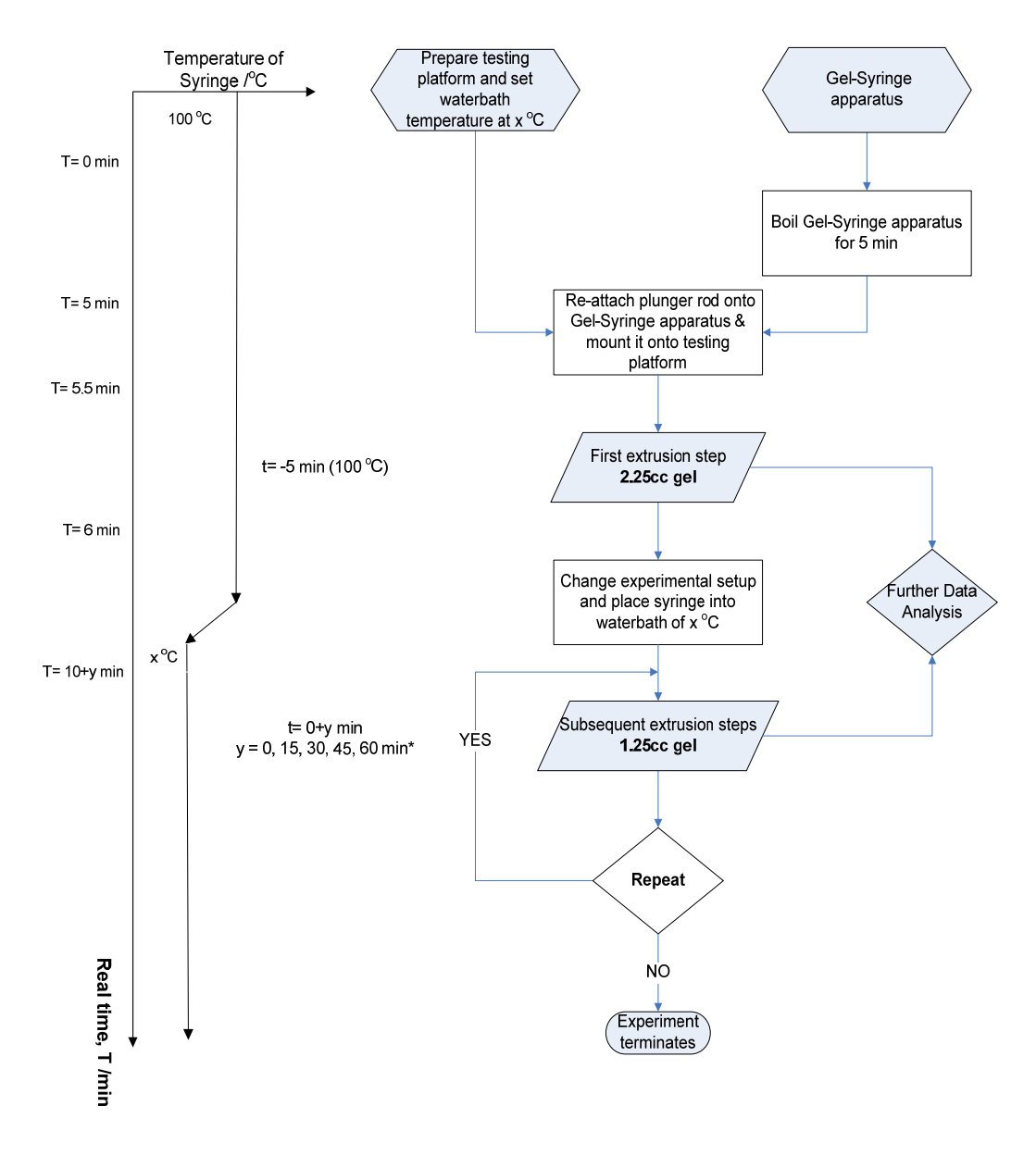
Volume [mm <sup>3</sup> ]	Displacement of hydrogel in syringe [mm]	Rate of displacement [mm/sec]	
1250	11.24	1.41	
2250	20.23	2.53	

# **Experimental procedure**

Figure 14 summarizes the experimental procedure. The testing platform and the syringe were prior prepared, a separate boiling waterbath tall enough to fully immerse the aluminium the syringe body and the ball valve was brought to boil. A timer was started T=0 min when the syringe loaded with hydrogel was placed into the boiling waterbath, as shown in Figure 13.



Figure 13: Boiling waterbath to melt the hydrogel encased in the syringe body



Waterbath temperature,  $x / ^{\circ}C = 25, 37, 50, 60$ 

\*Refer to Table 4, extrusion time points, y min, may vary, dependent on the experimental set

Figure 14: A flow diagram of the experimental procedure for hydrogel extrusion

After 5 minutes (T=5 min), the syringe was removed from the boiling water. The plunger stem was re-attached. Immediately, the syringe was inserted through the key-shaped hole of the aluminium stand, with the acrylic tank misaligned. The force reading at the load cell was reset to 0 N. The displacement controlled actuator arm was manually lowered till it

touched the flat base of the plunger stem. The MTS testing program was commenced. The actuator arm moved at the speed of 2.53 mm/sec, with increment displacement till 20.23 mm, translating to 2.25 cc total hydrogel extrusion. The measurement data obtained for this extrusion step were considered as the t=-5 min (100 °C) control value.

When the 8 seconds test program terminated, the syringe was removed momentarily to re-align the water filled acrylic tank waterbath and to restore the original height of the slotted base plate. The syringe was then inserted again through the key-shaped hole of the aluminium stand, with the cannula end protruding through the modified brass compression fitting (shown in Figure 15). A displacement rate of 1.41 mm/sec and a final displacement value of 11.24 mm, corresponding to 1.25 cc of hydrogel extrusion, were entered into the MTS program. At T=10 min, the next extrusion step was initiated. It was considered the t=0 min extrusion step.

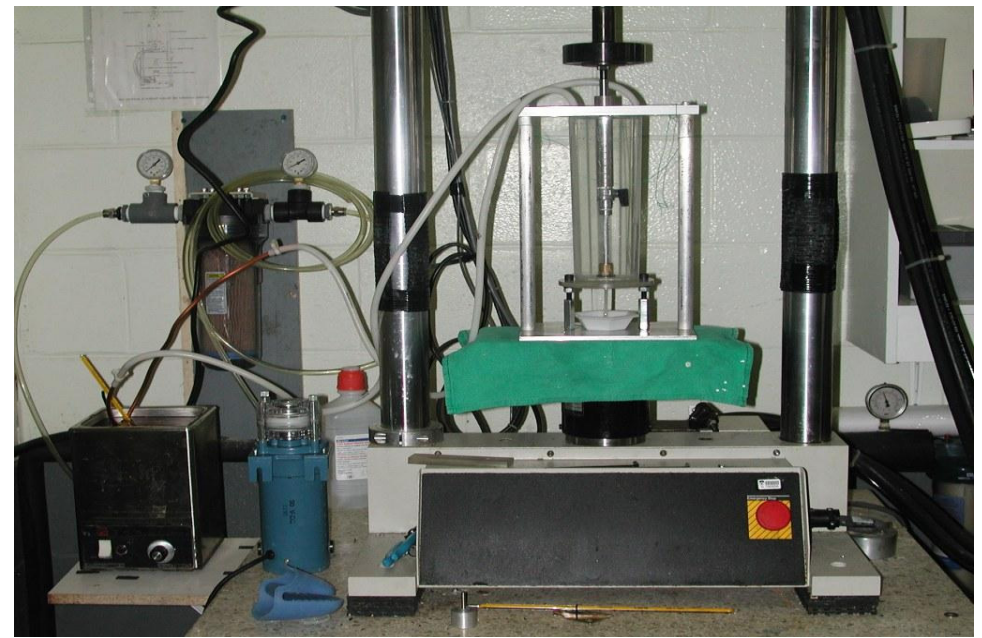


Figure 15: The hydrogel was being extruded from the bottom of the cannula

Referring to Figure 14, subsequent extrusion steps were initiated at 15, 30, 45 and 60 minutes extrusion set time points. The extrusion set

time points may vary, dependent on the hydrogel type and extrusion temperatures (see Table 3).

## Data analysis

The time, load and displacement data collected for each extrusion step was converted as follows into pressure values, using in Equation 4. The inner diameter of the syringe body measured 11.9 mm, therefore a constant cross-sectional area of 111.2 mm<sup>2</sup>. The cross section was multiplied with the final displacement of each extrusion step to calculate the extrusion volume. Pressure-volume curves for each hydrogel were plotted and the plateau values were extracted.

A table comprising plateau pressure values (when applicable) was tabulated. An experimental regression analysis on the plateau pressure values for each extrusion steps of hydrogel PVA121 Test 1, PVA14X Test 1 and Test 2, displayed for each extrusion temperature, was performed using Statsview®.

Pressure Equation:

$$Pressure = \frac{Force}{Cross-sectional Area}$$
 Equation 4

# 4.5 Curing Stiffness

To characterize the gelling rate of PVA121 and PVA14X, melted hydrogels were injected into custom made moulds and stored in different temperatures The objective of the experiment was to link the curing rate of the hydrogel, when exposed to different temperatures, by performing unconfined compression tests on the test specimen after specific incubation periods (IP).

## 4.5.1 Specimen selection and preparation

Table 5 and Table 6 showed total number of moulds required and the estimated number of hydrogel test tubes and the batch # of hydrogel used, at each incubation temperature. Three moulds per incubation period, temperature and hydrogel type were tested for its stiffness. The empty moulds were labelled as followed – "PVA121-4 8h", "PVA121-4 24hrs", "PVA121-4 72hrs" etc. "-4" and "-3" indicated the batch number of PVA121 used. The different batches of PVA14X were named PVA142 and PVA144 along with the IP in hours similar to that of PVA121. 3 incubation temperatures, 25 °C, 37 °C and 50 °C were chosen to investigate its effects on the curing rate of the hydrogel.

Table 5: Batch of hydrogel, total number of tubes and moulds required for PVA121

PVA121		Incubation	on Tempe	rature, IT	e, IT Moulds Estim		
		25 °C	37 °C	50 °C	required	Nos. of hydrogel tubes*	
0	Control (2w)	<b>3</b> PVA121-4	<b>3</b> PVA121-4	<b>3</b> PVA121-4	NIL	3	
Incubation Period, IP	8h	<b>3</b> PVA121-4	<b>3</b> PVA121-4	<b>3</b> PVA121-4			
	24h	<b>3</b> PVA121-4	<b>3</b> PVA121-4	<b>3</b> PVA121-4	27	7	
	72h	<b>3</b> PVA121-4	<b>3</b> PVA121-4	<b>3</b> PVA121-4			
	1w	<b>3</b> PVA121-3	<b>3</b> PVA121-3	<b>3</b> PVA121-3	18	5	
	2w	<b>3</b> PVA121-3	<b>3</b> PVA121-3	<b>3</b> PVA121-3	10	3	
Total*					45 + extras	15	

<sup>\*</sup>Assumption: Each tube of hydrogel provides materials for 5 castings

Table 6: Batch of hydrogel, total number of tubes and moulds required for PVA14X

PVA14X			on Tempe	Moulds	Estimated Nos. of	
		25 °C	37 °C	50 °C	required	hydrogel tubes*
IP	Control (2w)	<b>3</b> PVA144	<b>3</b> PVA144	<b>3</b> PVA144	NIL	3
Incubation Period, I	2h	<b>3</b> PVA142	<b>3</b> PVA142	<b>3</b> PVA142	27	
	8h	<b>3</b> PVA142	<b>3</b> PVA142	<b>3</b> PVA142		7
	24h	<b>3</b> PVA142	<b>3</b> PVA142	<b>3</b> PVA142		
	72w	<b>3</b> PVA144	<b>3</b> PVA144	<b>3</b> PVA144	40	5
	2w	<b>3</b> PVA144	<b>3</b> PVA144	<b>3</b> PVA144	18	
	Total*					15

<sup>\*</sup>Assumption: Each tube of hydrogel provides materials for 5 castings

45 moulds were required for testing each hydrogel. Five extra moulds were manufactured and casted so as to account for 'bad' castings that may occur ('bad' casting definition explained later). The casted moulds were placed in air-tight containers and kept at 100 % humidity, in

its respective incubation temperatures. This was achieved by placing the casted moulds on a dry platform which sat above a shallow reservoir of water.

## 4.5.2 Experimental setup

## Mould design and manufacturing

Brass, an alloy of zinc and copper, was used to manufacture the moulds. Referring to Figure 16, the assembled mould consisted of: (1) a larger brass tube cut at length, (2) a thin, slotted brass tube, (3) two ribbed, modified polypropylene plugs and (4) 2 brass washers of 12.7 mm ( $\frac{1}{2}$ ) diameter. In total, 50 moulds were prepared.

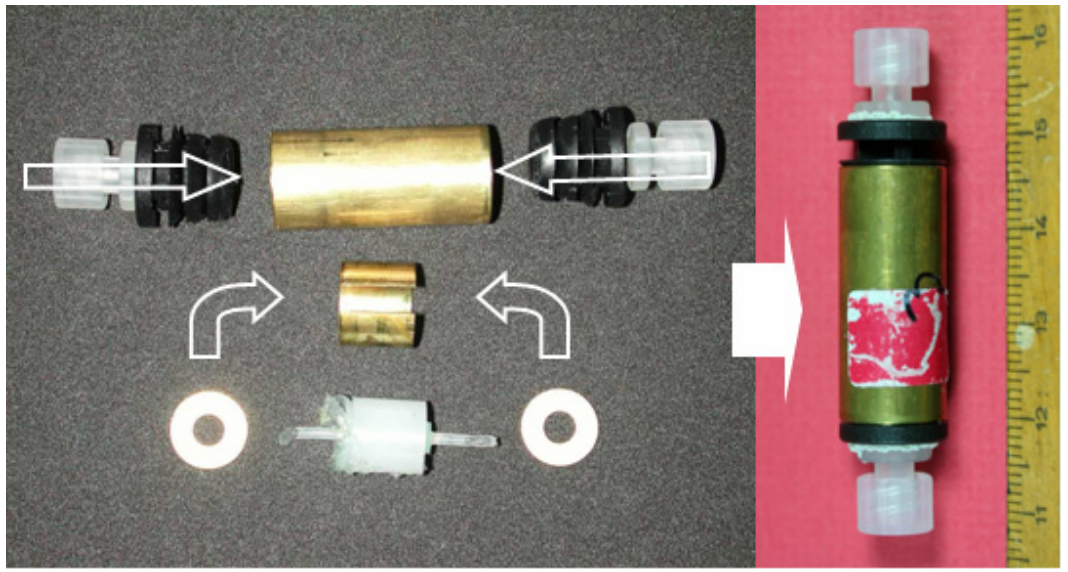


Figure 16: Brass cast assembly, before and after

The slotted brass tube was compressed until the lips of the slot met. It fitted snugly into the larger brass tube, defining an 11.9 mm inner diameter of the assembly. The 2 brass washers were inserted perpendicular to the longitudinal axis of larger brass tube where they rested against the ends of the inserted thin slotted tube, as shown in Figure 16. Lastly, the 2 ribbed plugs were inserted till they were pressing against the washers.

The large brass tube (Alloy 260) was drilled out to have an inner diameter (ID) of 12.7 mm (1/2"), with a length of 35 mm  $\pm 1$  mm. The thin brass tube was cut to a length 11.9 mm  $\pm 0.05$  mm. It had a wall thickness of 0.36 mm (0.014"). Its initial ID was 12.77 mm ( $\pm 0.01$  mm). To achieve an ID of 11.9 mm, a 4-flute carbide end mill of 7/64" ( $\sim 2.79$  mm) diameter was used to create the slot, as showed in Figure 17. A 7/64" slot was removed from the original circumference of the initial thin brass tube. The above value was calculated as the difference between the circumference of the original tube ( $\Pi * 12.77$  mm) and the targeted circumference of the thin, slotted brass tube ( $\Pi * 11.9$  mm).



Figure 17: Slotting the thin brass tube with an end-mill of 7/64" width

The one-time use of round, ribbed polypropylene plugs were selected to fit an 11.7–14.6 mm ID. A centered hole of 2.18 mm (0.086") was drilled through the plug and a polypropylene, female luer barbed-end fitting was inserted into it. An epoxy adhesive (3M Duo-pak Adhesive Cartridge, Dp-8005) was generously applied around the neck of the barbed-end fitting to glue the polypropylene parts together. Caution was taken to not to seal the central bore hole of the barbed-end fitting. It was left at room temperature to dry for 24 hours.

The brass washers had a 12.7 mm ( $\frac{1}{2}$ ") OD and 5.08 mm (0.2") ID. They rested snugly against the slotted brass tube's wall thickness. The washers also allowed for an easy push out action of the slotted brass tube. The center hole of the washers permitted the hydrogel to be injected into the mould.

A Medallion<sup>TM</sup> 10 cc syringe with a male luer orifice was the container used to melt and inject the hydrogel. The tang of the syringe was trimmed to fit into a standard 50 mL centrifuge tube. A wire was inserted through a 1 mm drilled hole near the tang and across the syringe. It keeps the Delrin<sup>®</sup> plunger in place, shown in Figure 18b. Figure 18a shows the syringe setup and Figure 18c shows the female-end Delrin<sup>®</sup> plunger piece, the complementing male-end stainless steel 304L plunger stem.

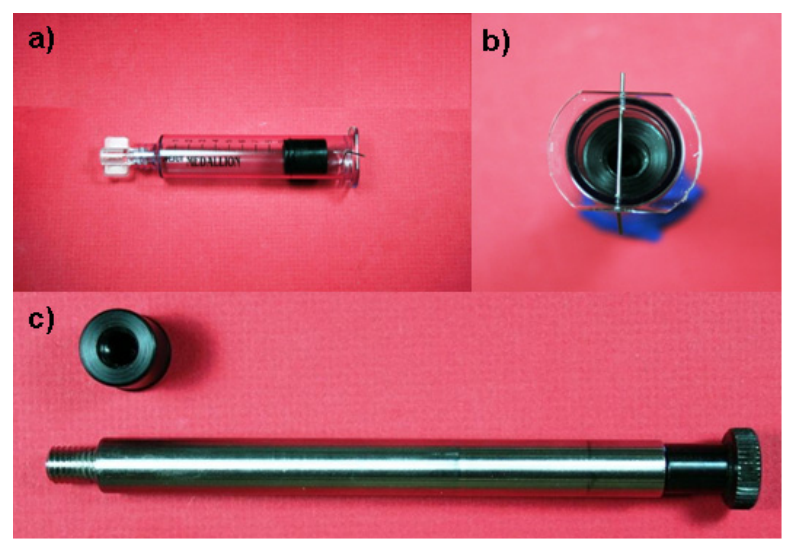


Figure 18: a) Longitudinal view of the syringe setup, sealed with a female-end luer-lock cap, a plunger and metal wire in place, b) Cross-sectional view of the metal wire locking the Delrin® plunger, c) Delrin® plunger system

## 4.5.3 Experimental Procedure

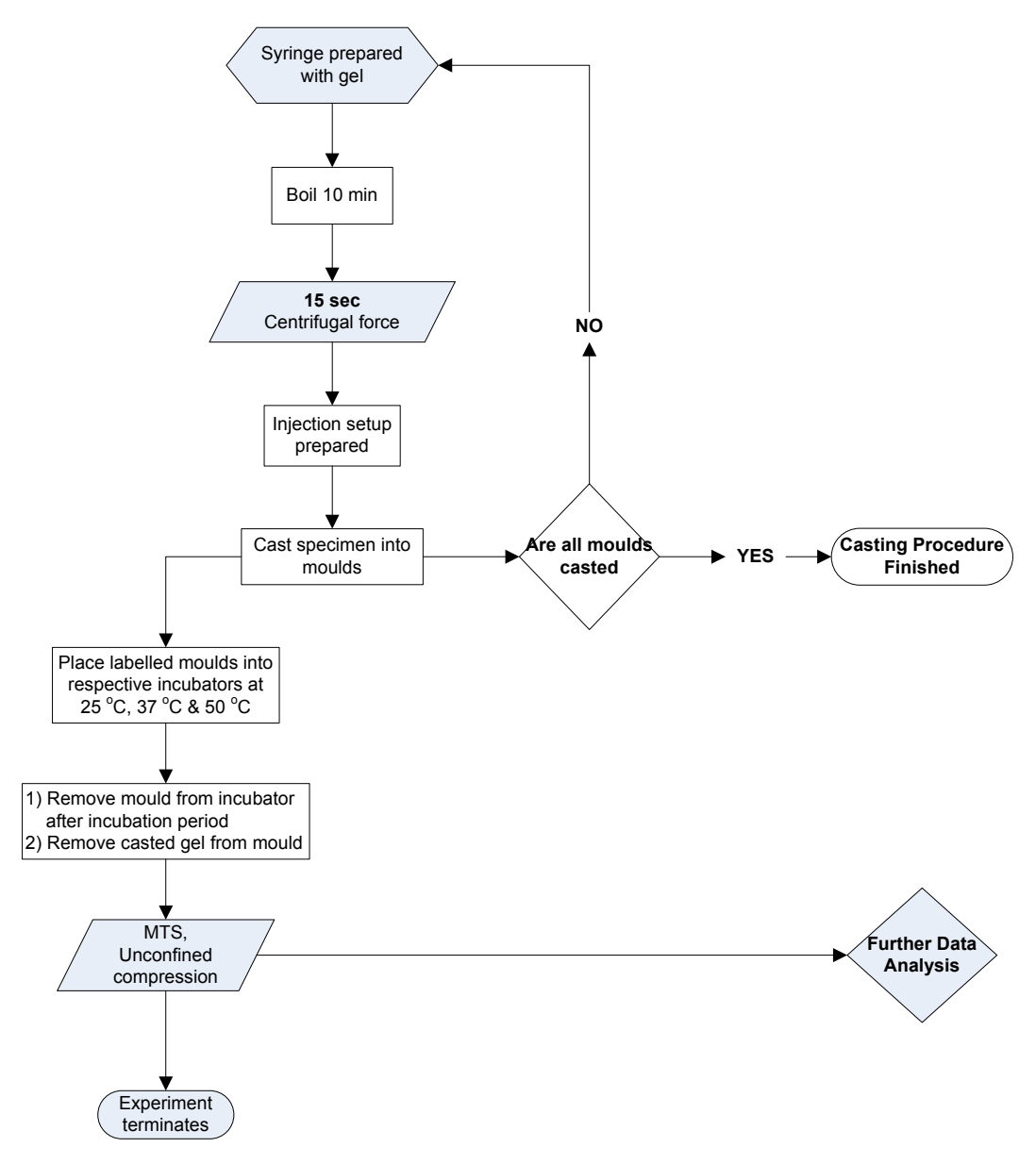


Figure 19: Flow diagram of the experimental procedure to characterize the curing hydrogel's stiffness over time

Figure 19 shows the experimental procedure of the hydrogel stiffness characterization over time. The hydrogel rod extracted from the test tube was cut into smaller pieces and fitted into a modified Medallion<sup>TM</sup> 10 cc syringe. The plunger was locked with a wire, and the luer-lock cap secured the orifice injection tip, as seen in Figure 18a.



Figure 20: Hydrogel locked within a medallion 10 cc syringe, in boiling waterbath

The filled syringe was placed upside down into the boiling water for 10 minutes (see Figure 20). Concurrently, a timer was started. At 3 minutes, a heatpack was placed in boiling water. At 9 minutes, a 50 mL centrifuge tube was added to the boiling water. At 10 minutes, the filled syringe was transferred upside down in a heated 50 mL centrifuge tube. The centrifuge tube filled with boiling water and the filled syringe was capped tightly.

Centrifugal force was applied to the centrifuge tube for 15 seconds. Any bubbles trapped within the melted hydrogel would rise to the syringe's tip. After which, the syringe was removed from the centrifuge tube, the thin wire was removed and the plunger stem was attached. The air at the syringe's tip is then forced out. Subsequently, the syringe, with the plunger attached, was mounted to the device featuring a threaded rod with a pushturning T-handle, as displayed in Figure 21.



Figure 21: The entire injection setup, including the syringe, plunger and the device with a threaded rod and T-handle

# **Casting procedure**

Gel casting commenced with the empty moulds labelled with the shortest incubation period. To start casting, the warmed up heatpack was wrapped around the syringe connected to one end of the mould while the other end was attached to a vacuum pump (see Figure 22).

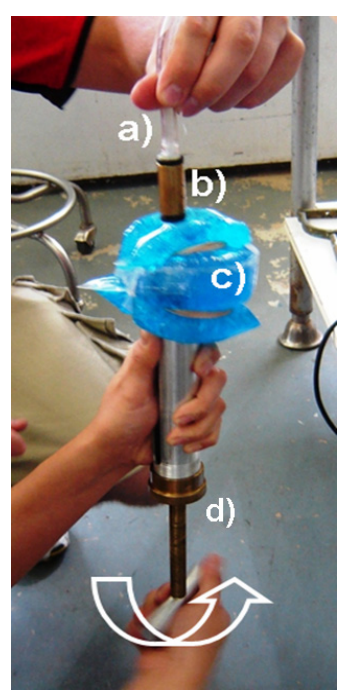


Figure 22: Extrusion of hot hydrogel into the mould connected to a vacuum pump Legend: a) hose connected to vacuum; b) mould; c) heat pack; d) device with T-handle

Slow half turns were made with the T-handle of the injection device to fill the moulds steadily and without trapping air. When the liquid hydrogel began to ooze out from the vacuum end of the mould, the mould was removed and capped with the female-luer caps (see Figure 16).

This procedure was used to fill all the moulds. Unmelted hydrogels that remained sealed in their respective glass tubes served as controls for this experiment. The casted moulds and unmelted control glass tubes were placed in incubators with the appropriate preset temperatures. The start incubation times were recorded for all casted moulds.

## Stiffness quantification procedure

The experimental procedure to measure stiffness in unconfined compression followed the protocol outlined in section 3.3 of this thesis. Instead of using sand-papered flat surfaces, 2 new flat surfaces with a dimple size of 1 mm depth and 5 mm diameter (Figure 23) were attached to the actuator arm and load cell respectively.



Figure 23: Gold pressers with 1 by 5mm holes

At time maturation, the moulds were removed from the respective incubators. Pliers were clamped onto the polypropylene plugs to forcefully pull them from the larger brass tube. Placed perpendicular to a firm surface, a metal rod of approximately 10 mm diameter and 50 mm height was inserted in the brass tube and pressed against the brass washer. Next, tapping the brass tube with a mallet pushed the thin, slotted brass piece out. The washers and the cast were retrieved from the mould without being damaged nor deformed.

Unconfined compression testing was then performed and the calculated stiffness data were averaged for each hydrogel type, incubation period and the incubator temperature. Plots were prepared showing the stiffness increase over time per hydrogel type and incubator temperature. The control value for the unmelted hydrogel was used as a benchmark for maximum stiffness.

# Chapter 5: Results

## 5.1 Swelling

Under free-swelling conditions, all 6 PVA121 specimen showed an exponential increase in weight percentage (wt%) for the initial 50 hrs of about 20-25 wt% (see Figure 24). After reaching a maximum swelling point, there was a sharp drop in weight percentage before gradually reaching weight percentage equilibrium. The hydrogel seemed to have reached equilibrium at about 1200 hrs (~7 wks) and 111-115 wt% compared to its initial weight, this before showing another slight dip at about 1400 hrs.

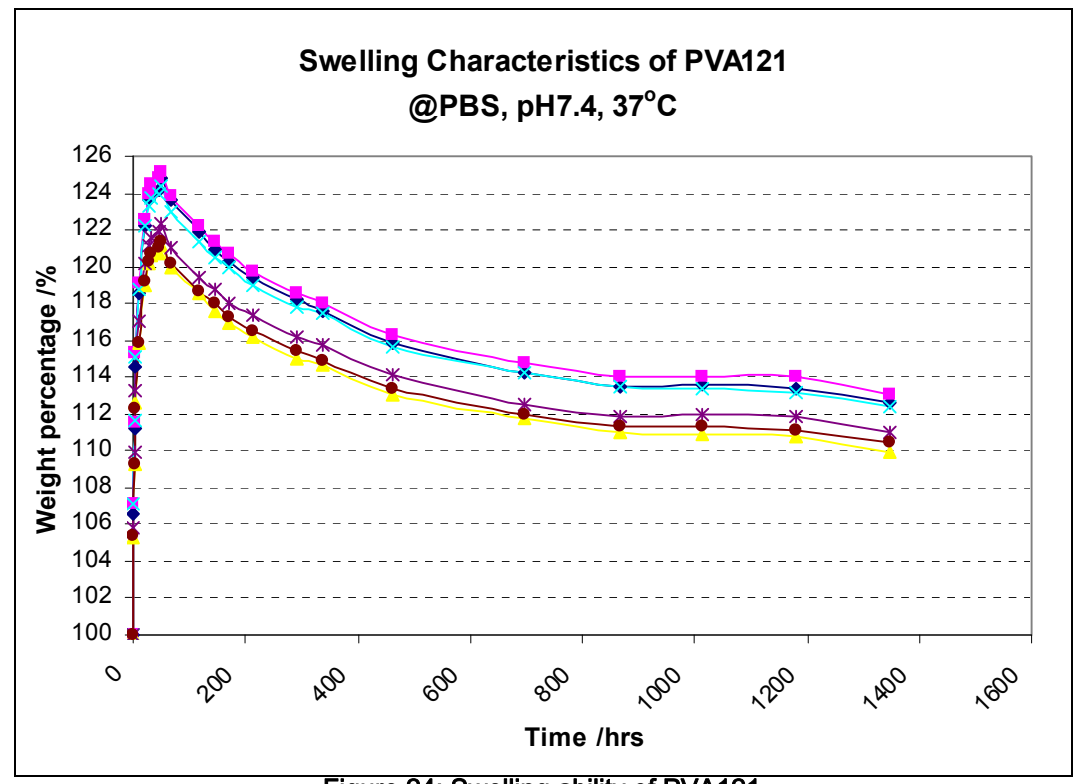


Figure 24: Swelling ability of PVA121

The swelling behaviour of PVA14X is shown in Figure 25. PVA14X reached its maximum swelling capacity, at an average of 116 wt% among its test specimen. PVA14X also reached its maximum swelling capability at approximately 50 hrs, similar to that of PVA121. Later, there was a

gradual loss of wt%, reaching equilibrium after about 800 hrs. Due to technical difficulties, swelling data collection stopped after 6 wks.

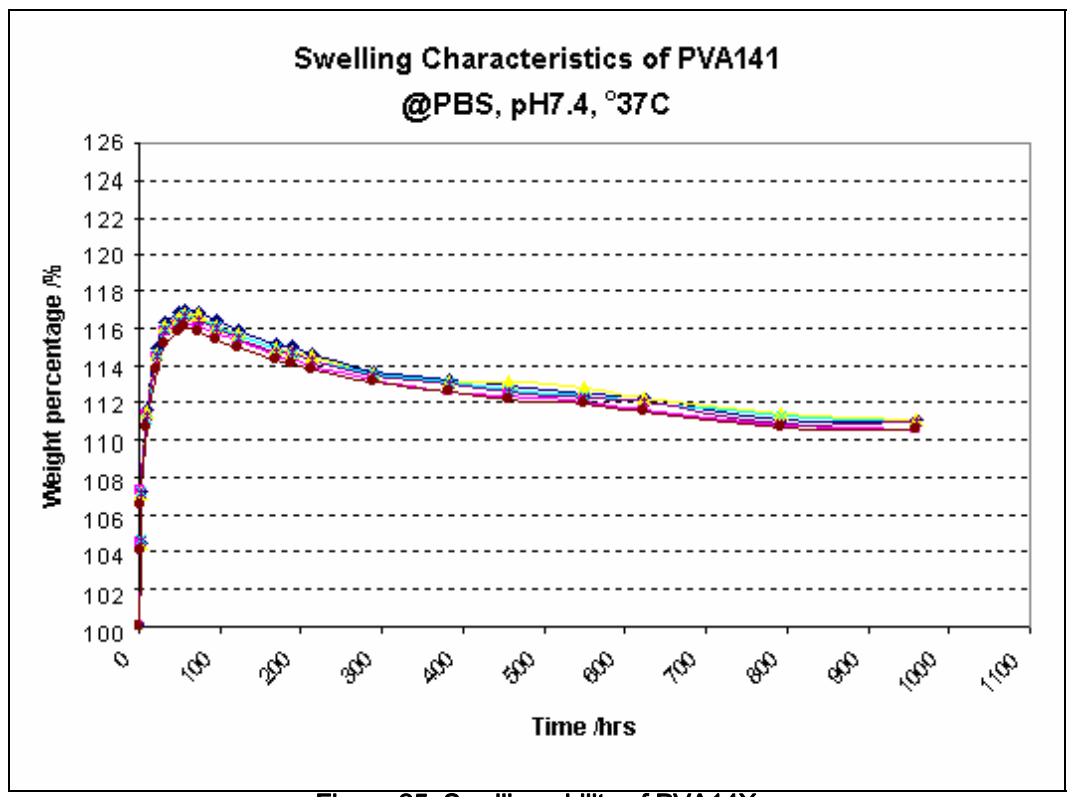


Figure 25: Swelling ability of PVA14X

Maximum swelling of PVA14X was less than that of PVA121. However, both hydrogels took approximately the same amount of time to reach similar wt% equilibrium of about 111 wt%. There was a larger variation in swelling capabilities observed in PVA121 compared to PVA14X.

## 5.2 Unconfined compression

Figure 26 showed a hydrogel specimen before and after 70 % compressive straining. All hydrogels exhibited significant permanent deformation after unconfined compression testing under high strains. Asides being physically deformed, wet marks were observed on the

contact surface of the sand paper, suggesting water extrusion from the hydrogel specimen during compression testing. Documentation was not pursued due to the difficulty in separating water loss due to natural evaporation from the hydrogel specimen (when handled in non-saturated air conditions) and water loss due to compression effects.

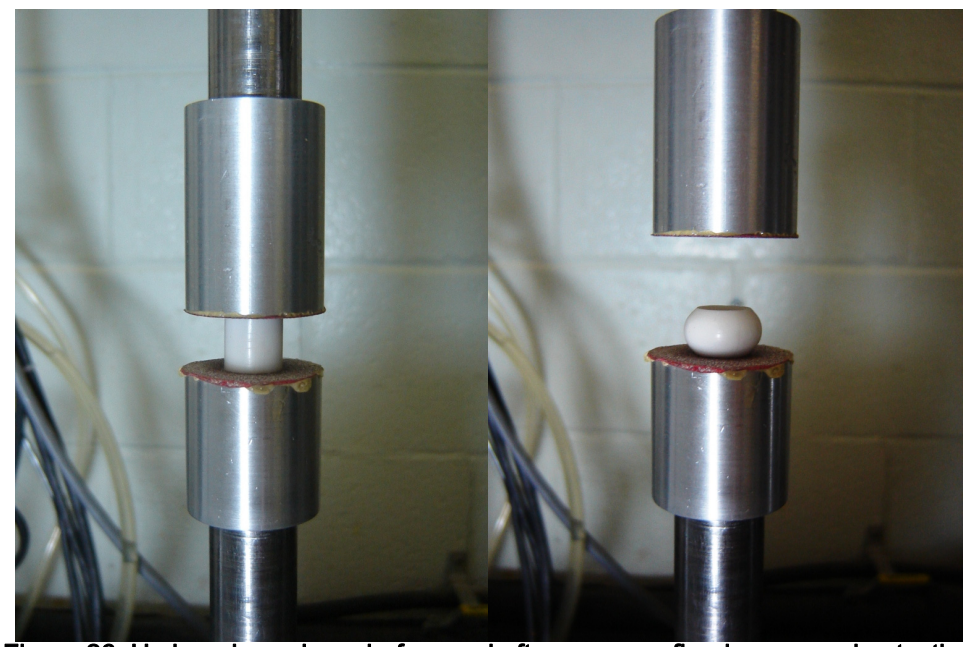


Figure 26: Hydrogel specimen before and after an unconfined compression testing

Stress-strain curves were plotted for specimen PVA121 and PVA14X, each tested at 0 hr (control), 48 hr, 4 wks and 8 wks. These stress-strain curves had non-linear responses. A typical example is shown in Figure 27.

The curve was linear to about 0.4 strain. Above 40 % strain, the line curved exponentially. Another phenomenon observed was a curve with two different gradients, also shown in Figure 27. In the left insert, the axes were rescaled and dotted tangential lines in red were drawn to highlight the phenomenon. This phenomenon seemed apparent in PVA14X but not for PVA121.

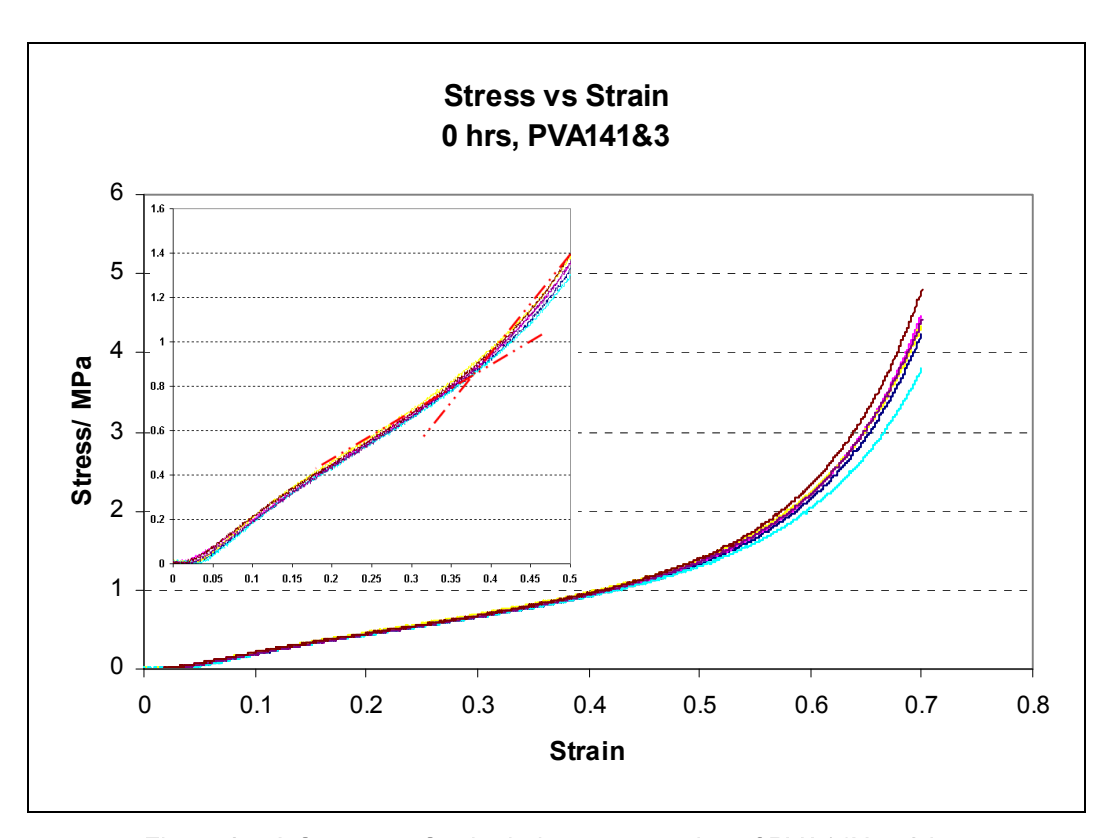


Figure 27: A Stress vs. Strain during compression of PVA14X at 0 hrs
The y-axis of the insert is rescaled to cover the range from 0-1.6 MPa, to accentuate the changes in gradient. The red tangential lines were added for comparison only

Figure 28 displays the modulus of elasticity of the PVA hydrogel as a function of compressive strain. The y-axis (modulus) was truncated at 20 MPa to focus the physiological relevant strain interval of 0.1–0.25. (For a complete view of the graphs, see Appendix).

These graphs exhibited an exponential increase in modulus of elasticity as the compressive strain increased. Results showed that at 0.1-0.25 strain, PVA14X and PVA121 hydrogels had an average modulus of elasticity of 2.0 MPa and 1.5 MPa, respectively. PVA14X hydrogels were found to be slightly stiffer than PVA121 hydrogels. Slight increases in the modulus of elasticity of both materials were documented for an 8 weeks period when swelling in PBS at 37 °C.

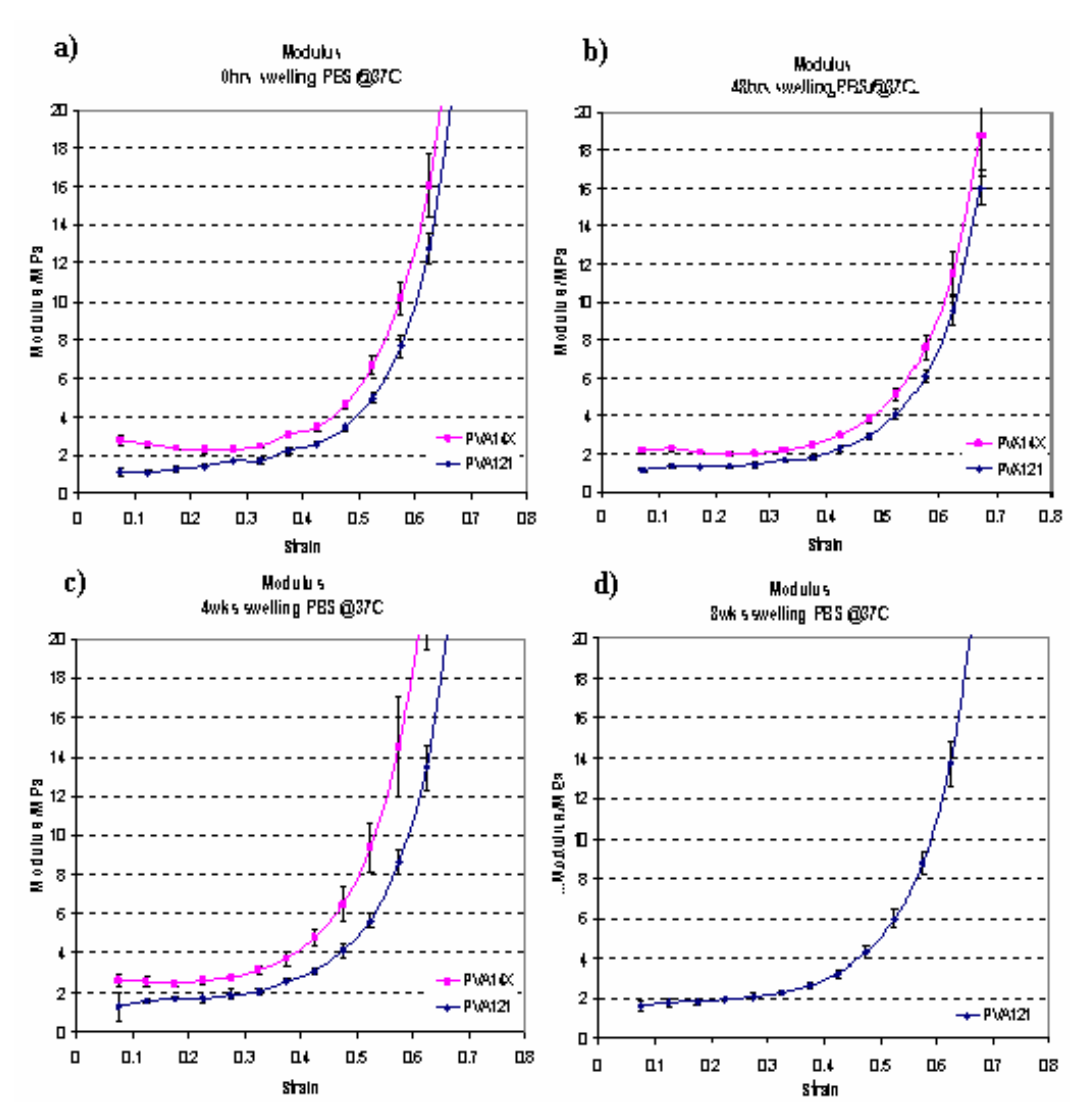


Figure 28: Modulus of elasticity for hydrogels plotted for different strain intervals of unconfined compression. All tests were performed after swelling in 37 °C PBS for different time intervals, except for the controls in 'a'.

Technical difficulties made it infeasible to complete the experiments for PVA14X. As a result, unconfined compression data at 8 weeks are missing. Nevertheless, the similar trend displayed on Figure 28a, 29b and 29c suggest a similar graph to be plotted for PVA14X in Figure 28d. In general, there were higher standard deviations calculated at very low strains. This larger variability will be further discussed in chapter 5.

As seen in Figure 28a, the stiffness of PVA14X at values between 0.1–0.25 strain seemed to decrease slightly from 2.7 MPa to 2.3 MPa. This downward trend was equally observed, although to a lesser degree,

for PVA14X in Figure 28b (48hrs) and Figure 28c (4 wks). Nevertheless, at high strains, all plots resume increasing exponentially.

#### 5.3 Gel extrusion

For each extrusion step, the pressure values were plotted against the extruded hydrogel volume. A sample of the resultant graph is shown in Figure 29. The graph was obtained for an extrusion test using a test tube from batch #1 of PVA121. Different extrusion steps for time points at t=-5 min (100 °C), t=0 min (50 °C), 15 min (50 °C), 30 min (50 °C), 45 min (50 °C) and 60 min (50 °C) were documented and subsequently plotted.

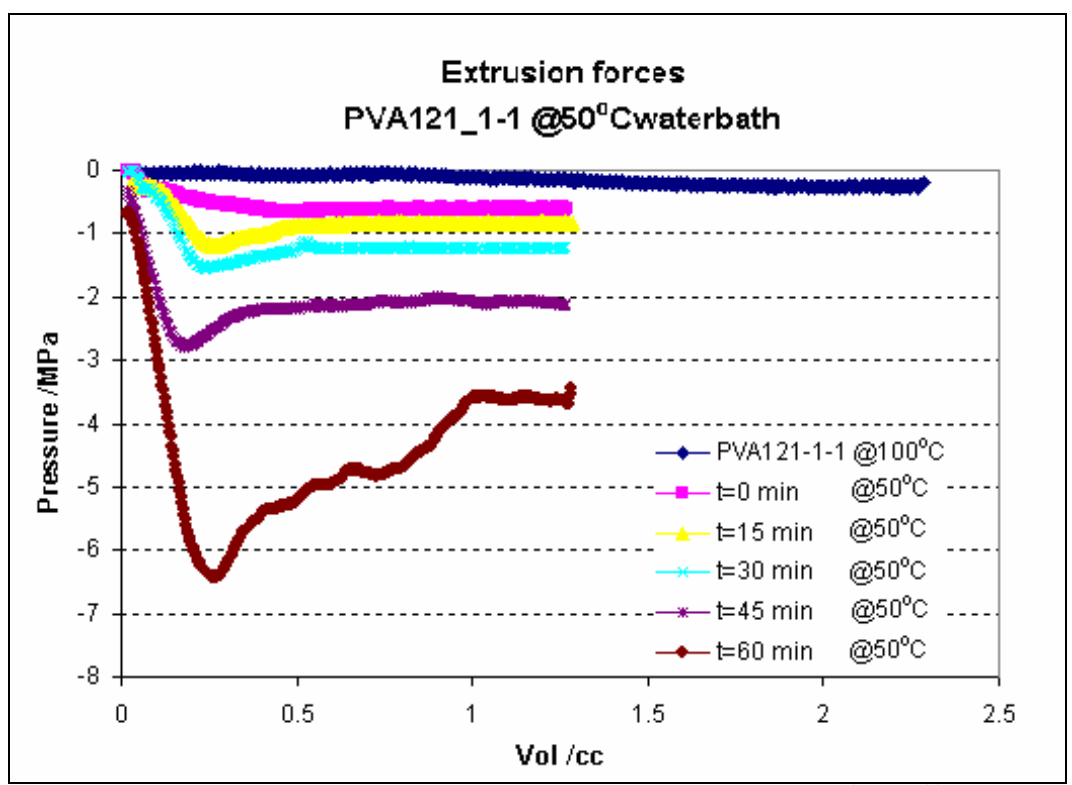


Figure 29: Pressure required to extrude hydrogel PVA121 at t = -5 min (100 °C), t =0 min, 15 min, 30 min, 45 min and 60 min in a 50 °C waterbath

The contents of six PVA121 hydrogel tubes were tested at ambient temperatures of 25 °C, 37 °C and 50 °C each. The content of each

hydrogel tube was used to measure a set of about 6 extrusion time points. For each ambient temperature group, 3 identical sets of extrusion time points were recorded. Therefore, 18 graphs similar to that of Figure 29 were plotted.

Extrusion tests for PVA14X were initially planned for only three repeats per temperature and time point (Test 1). The ambient temperatures were 37 °C, 50 °C and 60 °C. Thereby to increase the number of repeats was to 6, a second test series was performed 4 weeks later (Test 2). A total of 15 graphs similar to that of Figure 29 were plotted for PVA14X, thereby evaluating the sub groups for Test 1 and Test 2 independently.

For each extrusion step, the plateau value was noted from the pressure-volume graphs tabulated in Table 7 and Table 8. Especially for longer time points, it is often that the pressure volume plot did not exhibit a pressure plateau value. These time points were subsequently labelled as "Non-P" in the raw data sets. A typical example was illustrated in Figure 29, for the extrusion time point t=60 min.

Table 7 Plateau pressure recordings for PVA121

	Test 1					
25 °C	Pressure /MPa for 6 repeats					
Time /min	PVA121-1-1	PVA121-1-2	PVA121-1-3	PVA121-2-4	PVA121-2-5	PVA121-2-6
-5 (100C)	0.4	0.4	0.5	0.5	0.4	0.5
0	*Non-P	*Non-P	*Non-P	5.6	5.0	5.0
2				*Non-P	*Non-P	*Non-P
37 °C		Pre	ssure /MPa	a for 6 repe	ats	
	PVA121-1-1	PVA121-1-2	PVA121-1-3	PVA121-2-4	PVA121-2-5	PVA121-2-6
-5 (100°C)	0.4	0.5	0.4	0.4	0.4	0.4
0	1.0	1.1	1.0	0.9	0.9	0.9
5	1.8	2.4	1.6	1.3	1.2	1.2
10	15	16	6.0	3.1	2.2	2.8
50 °C	Pressure /MPa for 6 repeats					
	PVA121-1-1	PVA121-1-2	PVA121-1-3	PVA121-2-4	PVA121-2-5	PVA121-2-6
-5 (100°C)	0.3	0.4	0.5	0.4	0.5	0.5
0	0.6	0.6	0.6	0.6	0.6	0.7
15	0.9	0.9	0.9	0.7	8.0	0.8
30	1.2	1.2	1.3	0.8	1.0	1.2
45	2.0	2.4	2.6	1.1	1.3	2.0
60	6.5	7.5	9.0	1.5	2.3	6.0

<sup>\*</sup>Non-P indicates missing plateau pressure values (Refer to text for detailed explanation)

Table 8: Plateau pressure recordings for PVA14X

	Test 1			Test 2		
37 °C	Pressure /MPa for 2 repeats					
Time /min	PVA141_1	PVA141_2	N/A	N/A	N/A	N/A
-5 (100°C)	0.8	0.9				
0	*Non-P	*Non-P				
50 °C		Pre	ssure /MPa	a for 3 repe	ats	
Time /min	PVA141_1	PVA141_2	PVA141_3	PVA143-1E	PVA143-2E	PVA142-3E
-5 (100 °C)	0.6	1.0	0.9	1.0	0.8	0.9
0	1.7	1.8	2.2	15.0	10.0	5.6
2.5	1.8	3.7	5.9	*Non-P	*Non-P	*Non-P
5	9.4	14.0	*Non-P			
7.5	25.0	*Non-P	*Non-P			
10	*Non-P					
60 °C	Pressure /MPa for 3 repeat					
Time /min	PVA143_1	PVA143_2	PVA143_3	PVA143-1E	PVA143-2E	PVA142-3E
-5 (100°C)	0.8	0.8	0.8	1.2	1.0	1.1
0	1.3	1.3	1.3	1.5	1.5	1.3
5	1.6	1.7	1.8	2.1	2.1	1.6
15	2.4	3.7	1.3	5.5	5.1	2.7
30	7.1	*Non-P	*Non-P	*Non-P	*Non-P	*Non-P
40	*Non-P					

<sup>\*</sup>Non-P indicates missing plateau pressure values (Refer to text for detailed explanation)

Exponential curve regression analysis was performed using statistical software (StatsView®). The highest pressure value observed in non-plateau plots was used for subsequent regression analysis.

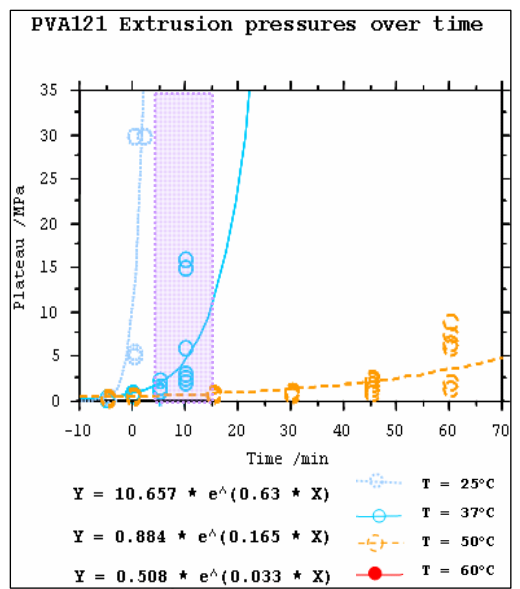


Figure 30: Regression plot of PVA 121 pressure plateau values over time at T = 25 °C, T=37 °C and T=50 °C.

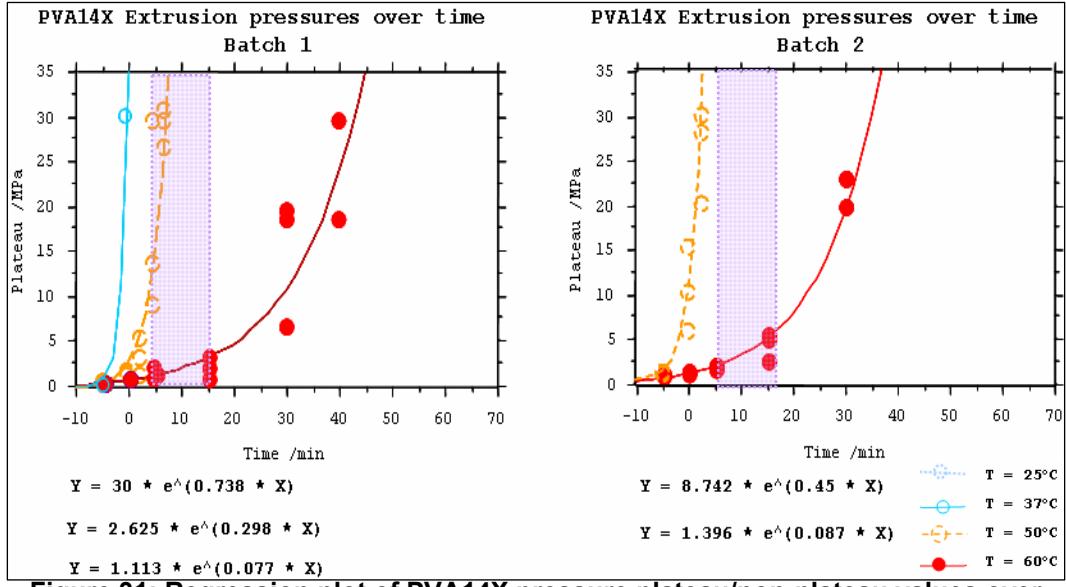


Figure 31: Regression plot of PVA14X pressure plateau/non-plateau values over time at T= 25 °C, T= 37 °C, T= 50 °C and T= 60 °C.

Regression plots, along with the exponential equations of the respective curve fits, are shown in Figures 31 and 32. Fitted curves depicting results from different extrusion temperatures were displayed. The light purple shaded time window (5-15 minutes) represents an ideal working time for physicians to inject the hydrogel into the intervertebral space. From these graphs, it was derived that hydrogel PVA121 is best injected at a temperature of approximately 37 °C. Similarly, PVA14X during Test 1 was best injected at a temperature of approximately 50 °C, while Test 2 is best injected between temperatures of 50 °C and 60 °C.

## 5.4 Gel Curing

A cured cast, still encased in the inner slotted brass piece, is shown in Figure 32a. A solid string of hydrogel extending from the nipple end of the cast was cut off using the brass washers as a guide for the cutting blade.

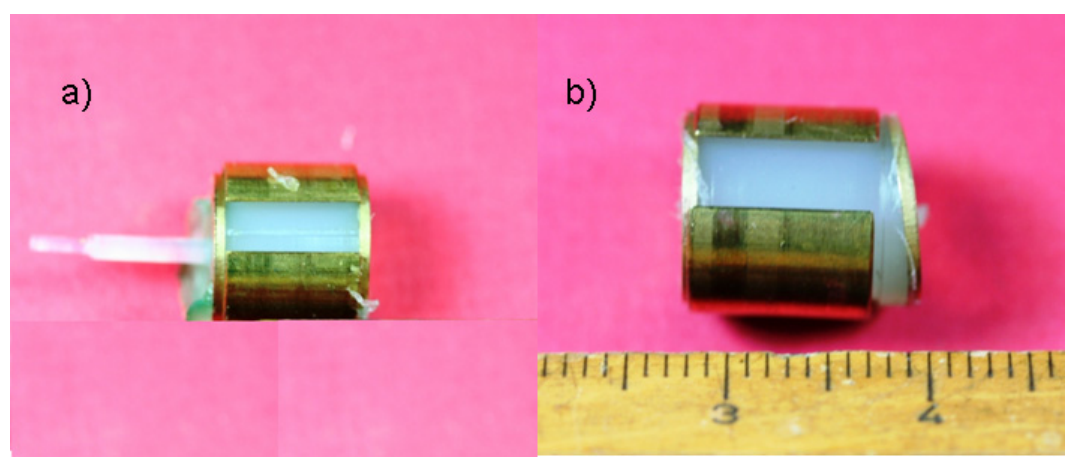


Figure 32: a) Encased cured hydrogel b) Cured hydrogel with a sub-optimal shape

Both Figure 32a and Figure 33b show casts with green stains on few surfaces of the hydrogel. About half of the PVA121 hydrogels exhibited this stain. None of the affected casts were completely coated thoroughly by the stain. Hydrogel PVA14X did not show any stains when removed from its casts.

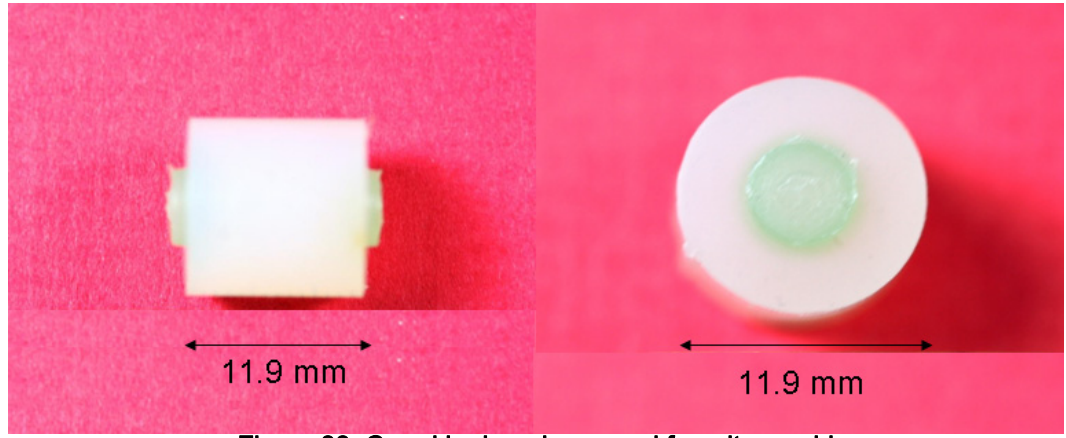


Figure 33: Cured hydrogel removed from its mould

Figure 33 shows typical images of a cured hydrogel specimen removed from the slotted brass tube. By default of the mould size, the resultant test specimen had a similar height and diameter of 11.9 mm. All specimens had a concentric nipple protruding 1 mm from both flat ends of the specimen due to the mould of the washers.

All heights of cured specimen which were not consistent with Figure 33, but have perpendicular surfaces to the longitudinal axis of specimen were measured thrice and averaged across (not including the height of the nipples).

An example of a discarded cured specimen is shown in Figure 32b. It has a slanted angle face instead of the normal 90° angle. Another form of a discarded cured specimen was due to trapped air bubbles within the mould, shown in Figure 34. When the size of the air-bubble was too large relative to the size of the test specimen, it compromised the stiffness of the specimen significantly. Subjective judgment was made whether the specimen with trapped air bubbles was still utilized for stiffness data collection.



Figure 34: An example of an air bubble 3 mm in diameter entrapped in a cured gel sample excluded from further testing

Figure 35 to 39 summarize the modulus of elasticity determined during unconfined compression the results of hydrogel types PVA121 and PVA14X, for different time intervals and different curing temperatures. For graph clarity purposes, the standard deviation from the three repeats measured for each condition are not shown in the figures. Its standard deviation had an average of only about 0.1 MPa. A table listing all standard deviations was included in the appendix.

PVA121 and PVA14X showed a steady increasing modulus across the two weeks of curing. PVA14X displayed a faster curing rate, reaching about 70 % of the control stiffness within 72 hours, while PVA121 reached about 50 % of its control stiffness only after 1 week of curing.

The curing rates of PVA121 and PVA14X were found to be temperature dependent. Both PVA121 and PVA12X had the fastest curing rate when stored in a surrounding temperature of 37 °C. Exposure to ambient temperature at 25 °C resulted in the slowest curing rate for PVA121. For PVA14X, it was non-conclusive if 25 °C or 50 °C ambient temperatures gave rise to the slowest curing rate.

Comparing the graphs between PVA121 for 10-20 % strain and 20-30 % strain did not show significant differences in the curing rate. PVA121 did not reach its original stiffness, marked by the control, after a period of 2 weeks. On the other hand, PVA14X reached its original stiffness by 2 weeks.

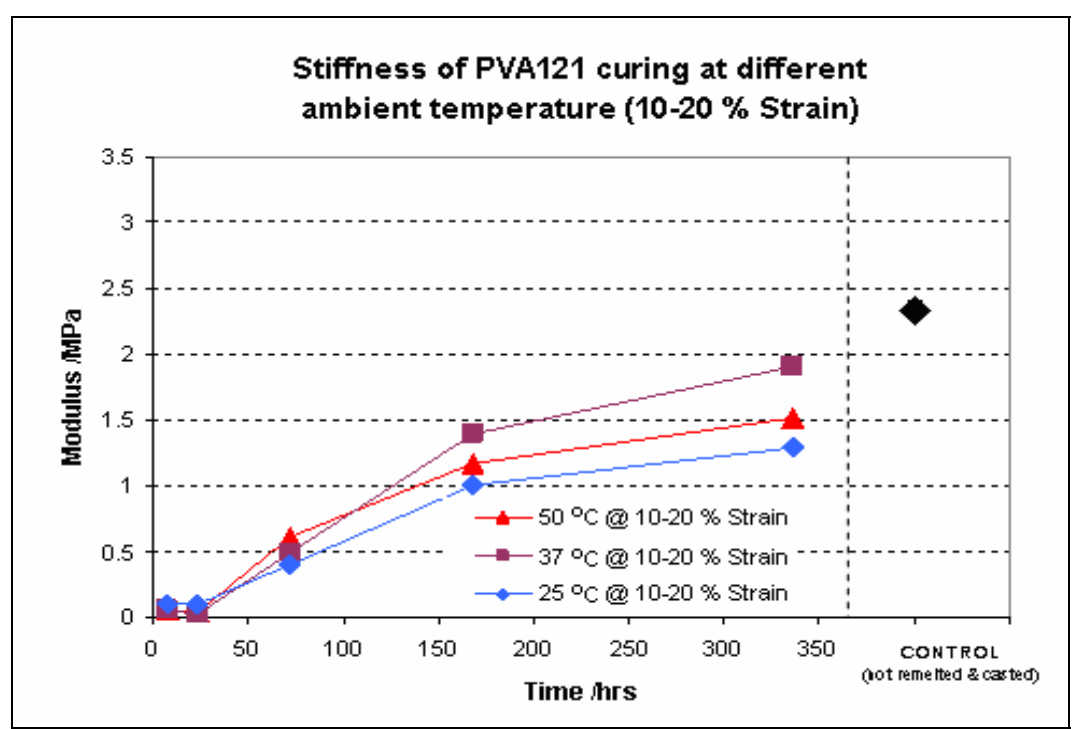


Figure 35: Modulus change of PVA121 measured at 10-20 % strain over a period of 2 wks curing. The control value is obtained from a similar hydrogel that was not melted

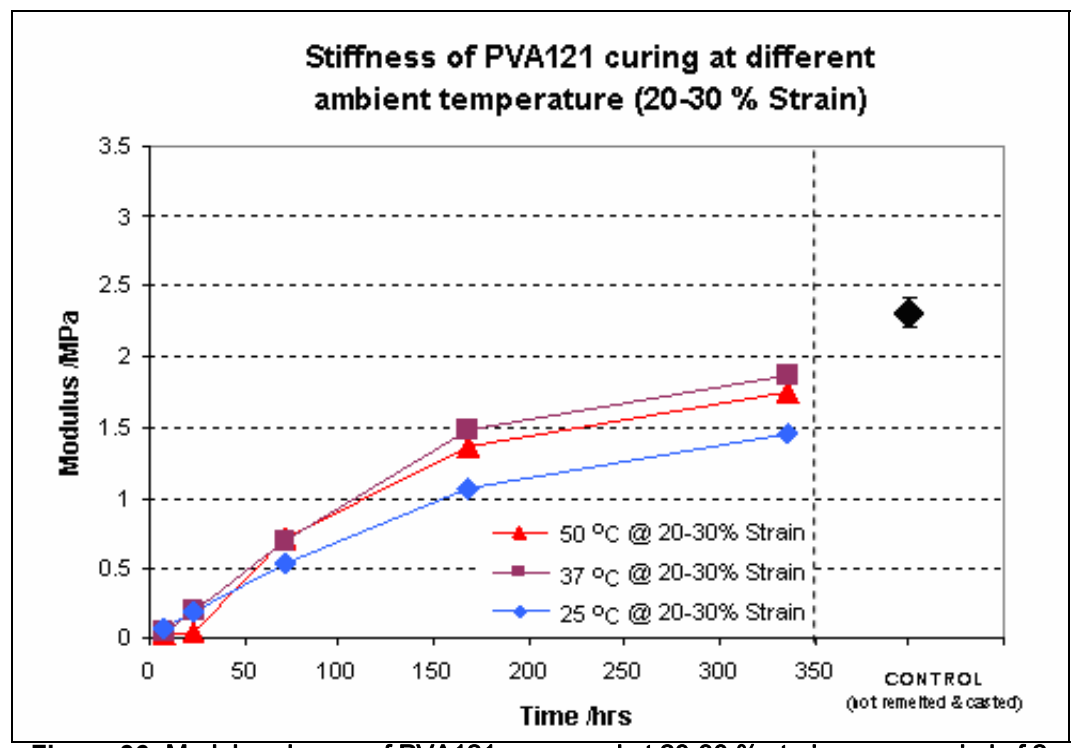


Figure 36: Modulus change of PVA121 measured at 20-30 % strain over a period of 2 wks curing. The control value is obtained from a similar hydrogel that was not melted

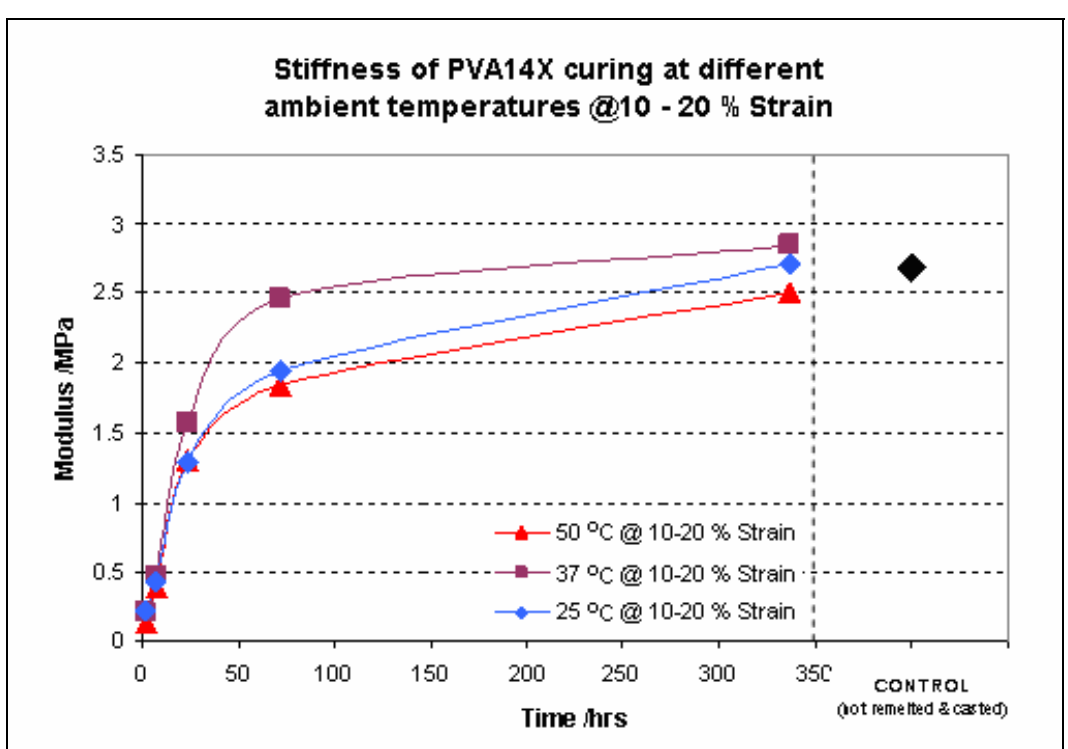


Figure 37: Modulus change of PVA14X measured at 10-20 % strain over a period of 2 wks curing. The control value is obtained from a similar hydrogel that was not melted

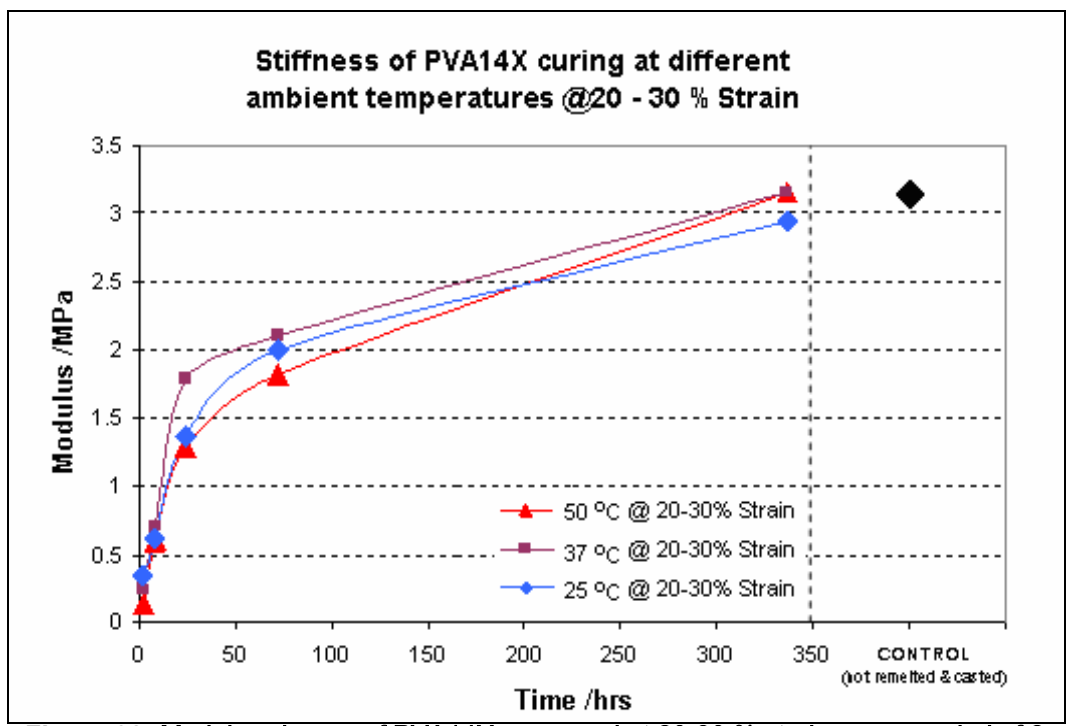


Figure 38: Modulus change of PVA14X measured at 20-30 % strain over a period of 2 wks curing. The control value is obtained from a similar hydrogel that was not melted

# Chapter 6: Discussions

## 6.1 PVA hydrogels

PVA14X had a 17 wt% of barium sulphate added to the gel phase to make the hydrogel radiopaque. Radiopacity is a desired feature for a NP replacement material because it allows the verification of shape and positioning of the injected hydrogel within a patient, using the non-invasive technique of X-ray. However, more mechanical tests should be pursued to guarantee the biocompatibility *in-vivo* and inertness of the added filler material to the curing process of the PVA hydrogels.

## 6.2 Swelling

Swelling tests of all 6 PVA121 specimen were conducted concurrently. The chosen sample size and swelling duration of 8 weeks in physiologic solution were deemed reasonable to observe the material's swelling behaviour. PVA14X (59.4 wt% of water) consist of a lower water percentage content compared to PVA121 (65.8 wt% of water). Screening results indicated that lower initial water weight percentage led to lower swelling capability. Therefore, it was not surprising to discover that PVA14X had a somewhat lower swelling ability.

PVA121's seemingly sharp drop in weight percentage (see Figure 24) could have been accentuated due to the lack of in-between data points between 51 hrs and 68 hrs. Nevertheless, extra data points would not have made the relative maximum to disappear.

Another somewhat unexpected finding was the last data point collected at 8 weeks for PVA121. After reaching an equilibrium between 5 to 7 weeks (900-1200 hrs), the 8-week data point was again lower. Unfortunately, hydrogel weights were not monitored further and therefore can not confidently comment on the unexpected 8-weeks value.

It was discovered in the screening tests of earlier hydrogel formulations that leaching (i.e. net loss of dry weight) may have occurred from the specimen. The net loss of dry weight was also suggested due to the dissolution process. Although swollen PVA121 and PVA14X hydrogels had shown to maintain weights over 8 weeks, there is a possibility that improved formulations had only delayed the leaching or dissolution process.

Further analysis was not pursued to determine the cause of weight loss, as the focus of this research is to determine the hydrogel's suitability as a NP replacement. Furthermore, additional costs and time, such as mass spectrometry usage and re-designing experimental protocols, will need to be devised and evaluated. It is recommended that further analysis can be done for future tests.

## 6.3 Unconfined compression

In a normal intervertebral disc, in addition to preventing the lateral expansion of the NP, compressive loads are also cushioned partially by hoop stresses in the annulus. Therefore, a more realistic testing of the hydrogels to determine a compressive modulus should be done using a semi-confined compression testing protocol. However, the complexities to mimic a realistic model of the confining effect of the annulus were overwhelming. Others have used various synthetic materials to serve as a model simulating the annulus for confined compression testing [52;60;80]. Nevertheless, using an unconfined compression test still gave valid data, as a comparison between different hydrogels, time period, temperatures, etc. Joshi *et al* [52] used test specimen 1:1 height to diameter ratio (6 mm by 6 mm) and unconfined compressed them at strain rates of 100 %/min or 1.67 %/sec. Our results, obtained at 1 %strain/sec (e.g. Figure 27), one expect to have will have a slightly lower resultant modulus.

A linear relationship derived from the stress vs. strain data up to about 40 % strain suggests that the material has exhibited elastic behaviour in this range. However, the relationship became exponential after 40% strain. A few underlying factors contributed to this course.

- 1. Plasticity occurred within the specimen.
- 2. The cross-sectional area in contact with the pressers increased as the plug becomes more compressed. However, our calculations did not accommodate for this change in area.
- During compression, there is friction opposing the lateral spread of the material against the contact surfaces of the MTS machine. This force is contributing to the inaccuracy. The magnitude of error level increases significantly as the plug becomes progressively compressed.

A few factors that can explain the unstable base value for the compressive modulus between 7.5-17.5 % strains are discussed.

- 1. Due to the elasticity of the hydrogel, there is a period of load accommodation before load readings from the MTS machine become reliably raising. Therefore, deciding on the initial specimen height is subjective. This variability biases overlaps into the later calculations of the material's compressive modulus.
- 2. The initial height measurement using digital callipers is subjective as the hydrogel has a significant degree of elasticity. This equally contributes to error in the calculation of strain.

The increasing standard deviation after 40 % strain is attributed to the accentuation of error, from the variability in initial height measurements. Assuming a  $\pm 5$  % initial height measurement error, compressive displacement to 70 % of its initial height translates to an error of 5 % over the remaining 30 % specimen height, or an approximate of 15 % error.

The nucleus pulposus has a biphasic nature, where it exhibits both fluid and solid-like properties [27]. This nature can explain the

phenomenon of the higher than expected compressive modulus at low strain values in the range of 7.5 % to 15 %. An example was illustrated earlier in Figure 27. The PVA hydrogel is composed of water and polyvinyl alcohol-chains. It is hypothesised that the initial gradient displays the combined modulus of both the plug's solid and water phase. Above a critical compressive stress, the solid phase takes over to support the external stress while the water is possibly displaced from the specimen, resulting in a lower gradient.

#### 6.4 Gel extrusion

To successfully inject an in-situ curing hydrogel through a thin cannula, one needs to find a compromise between hydrogel solidification rate, extrusion pressures required and temperature of the hydrogel at the time of injection. A hand-held injection applicator will not be suitable for extrusion pressure values higher than 10 MPa. Therefore, a customised experimental design was designed, built and tested to optimize the underlying injection parameters.

## 6.4.1 Experimental design

A 13.5 cm length, 8-gauge injection cannula (inner diameter of 3.2 mm) was used for the extrusion experiment. The dimensions are derived from requirements of the spinal surgical procedure. Injection temperatures of 25 °C, 37 °C, 50 °C and 60 °C were chosen to characterize the relationship between temperature and extrusion pressures. These temperatures were considered to be within the range of temperatures that will not cause heat damage to tissue.

For the syringe, the chosen material needs to have high mechanical strength, a high thermal conductivity, as well as relatively good resistance against water corrosion. Referring to Table 9, copper and

aluminium both have the desired high thermal conductivities. Stainless steel is stiffer than aluminium but has a much lower thermal conductivity and is harder to machine. Surface oxidation of aluminium reduces its thermal conductivity, but improves corrosion resistance. Polycarbonate is relatively stiff, resistant to corrosion and translucent. Translucence will allow one to see the content within the tube. However, polycarbonate, like most polymers have very low thermal conductivity. Aluminium was chosen as a trade off between mechanical strength, thermal conductivity and corrosion resistance.

Table 9: Thermal conductivity of different materials at 20 °C

	Thermal conductivity at 20 °C W/mK
Aluminium	237
Copper	390
Stainless Steel	16
Aluminium Oxide	30
Polycarbonate	0.2

From http://www.sas.org/engineerByMaterial.html

The 5-minutes waiting period chosen for to cool down the syringe in the temperature controlled waterbath was based empirically on the cooling rate that occurs through heat transfer from the aluminium to the surrounding waterbath. To simulate the cooling rate for PVA hydrogel in the experimental syringe, an aluminium hollow tube with an approximate length of 130 mm, an ID of 14 mm, and a wall thickness of 1.3 mm, was used. Its bottom end was sealed with a rubber cap. This make-shift aluminium tube was heated up to 100 °C (immersed in a boiling waterbath) and then transferred to another waterbath with the lower temperature (E.g. 37 °C). The water temperature inside the make-shift aluminium tube was recorded off a thermometer reading (see Figure 39).

Water medium was used to substitute hydrogel to determine the approximate thermal conductivity of hydrogel. Preliminary tests showed that this PVA hydrogel quickly looses its water content and decomposes

when heated in non-saturated air conditions. Liquid PVA hydrogel is hypothesized to have lower convection properties than water. Due to the high water content in the PVA hydrogel, its heat capacity is expected to be only slightly lower than that of water, therefore temperature equilibrium would be reached in a time span comparative to water, or possibly slightly longer.

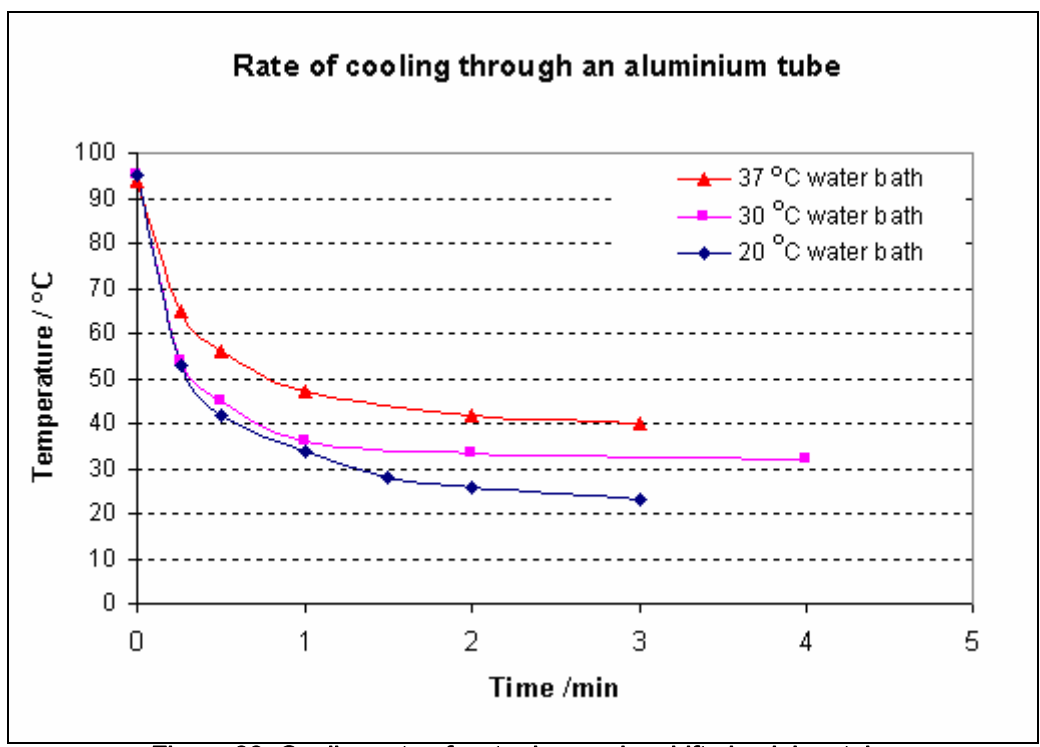


Figure 39: Cooling rate of water in a make-shift aluminium tube

#### 6.4.2 Extrusion volumes

A 2.25 cc extrusion volume at the initial extrusion step (t = -5 min  $(100 \, ^{\circ}\text{C})$  was chosen because extra volume was required to fill the empty cannula with hydrogel. A steady state force was achieved when the input volume into the cannula equals the volume output. Hydrogel left within the syringe was exposed to a similar ambient temperature comparable to the syringe body. The entire syringe body as well as most of the cannula were immersed in the temperature regulated waterbath. Although the very tip of the cannula was exposed to room temperature, this contribution was

considered to be minimal when measuring extrusion forces. Subsequent extrusion steps required a 1.25 cc volume to reach a steady state force (i.e. plateau force values).

## 6.4.3 Choice of extrusion temperature

Extrusion pressures were tested at 25 °C, 37 °C, 50 °C and 60 °C. 37 °C follows the normal body temperature of a patient. 25 °C was decided from trial and error. Below 25 °C, the extrusion pressures increased too rapidly to be useful for a controlled hydrogel injection.

50 °C and 60 °C are the upper temperature limits that human tissue, for short periods of time, can withstand without heat damages. Literature suggests that rate of skin burn depends on two interdependent factors: temperature exposure and contact duration; skin contact with temperatures above 50 °C leads to first degree burns within a few seconds [81;82]. Intolerance to higher temperatures grows exponentially.

It is projected up to 4 cc hydrogel is needed for injection. Although 60 °C is ten degrees above literature values, it is assumed that tissue tolerance will be higher in-vivo, aqueous tissue environment. The relatively small heat capacity from the injected hydrogel can be quickly dissipated to the surroundings aqueous intervertebral tissues; hence we think 60 °C for the hydrogel temperature at the time of injection can be tolerated with no relevant tissue damage.

#### 6.4.4 Extrusion results

All extrusion steps ran for 8 seconds. The initial extrusion step at a higher volume resulted in a higher velocity (2.53 mm/sec compared to 1.41 mm/sec). A higher velocity results in a higher extrusion pressure. However, velocity measured for all initial extrusion steps only served as a control across the entire experiment. It showed that both, PVA121 and PVA14X, when melted to 100 °C, had similarly low pressures of

approximately 1 MPa. Because of the higher velocity, the pressures recorded at subsequent extrusion steps are overestimated. However, the above inaccuracy has no implications on conclusions stated for the ideal injection temperature.

Pressure readings for otherwise similar conditions demonstrated large variability. Storage time of the PVA hydrogel also seem to affect its material properties and related extrusion pressures. Further investigation would be required for a more conclusive assessment of long-term storage effect on extrusion pressures.

Higher initial pressures were required to overcome the inertia of flow before a plateau value was reached, as seen mainly for t=15 min, 30 min and 45 min time intervals in Figure 29. The pressure spikes became more pronounced as the gelling time and hydrogel viscosity increased. Another explanation for the pressure spikes could be due to the lower temperature exposure at the tip of the cannula, so that higher forces were required to extrude the "colder" hydrogel at the cannula tip before the "normal" temperature hydrogel was extruding.

Hydrogel extrusion at lower viscosity resulted in a plateau pressure being reached within the 8 seconds of testing. At higher viscosities, towards the transition period where the liquid phase hydrogel solidifies, uneven pressures were recorded during extrusion (example seen in Figure 29 at t=60 min). Uneven pressure recordings suggested the occurrence of shearing effects. Higher forces were required to shear the "solid" portions through the cannula step present at the transition of the larger ID of the aluminium tube into the smaller ID of the cannula.

## 6.5 PVA hydrogel curing

It is essential to understand the rate of PVA hydrogel curing after injected it into the intervertebral disc space. This curing rate affects the "resting period" of a patient required, before he can resume daily activities

without compromising the hydrogel's integrity. To function as a nucleus pulposus substitute, the hydrogel does not need to reach 100 % of its final stiffness. However, the hydrogel should attain a significant percentage of stiffness within a reasonable amount of time, so that the extrusion risk in the context of, for instance, an overnight-stay surgery, will be manageable.

## 6.5.1 Experimental design rational

Two prototype generations of hydrogel moulds were tested before deciding on the final design. Hydrogel casting mould design needed to be easy enough for production in quantities of 50. The first prototype (see Figure 40) was made from 3 circular pieces of solid pieces, with the center cavity to have an 11.9 mm height and diameter hole. The other two pieces, acting as covers, had a center hole drilled to create a passageway for hydrogel injection. Six peripheral and lined-up holes served to assemble the parts with nuts and bolts. Unfortunately, cured hydrogel stuck to the walls of the moulds, making removal difficult without permanently deforming the hydrogel specimen.

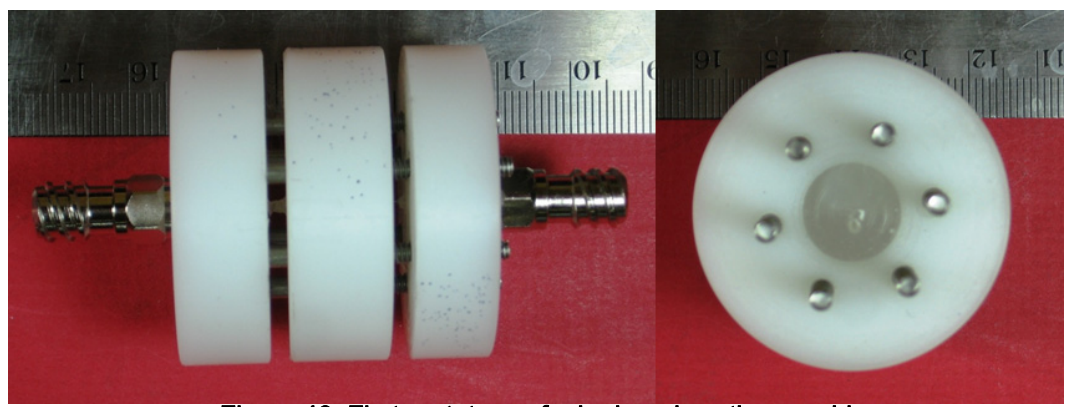


Figure 40: First prototype of a hydrogel casting mould

The second prototype in Figure 41 was the precursor to the final concept using double layered casting: a flexible, inner cast and a structural outer cast. The two end caps were similar, one serving as the injection and the other as the vacuum portal.

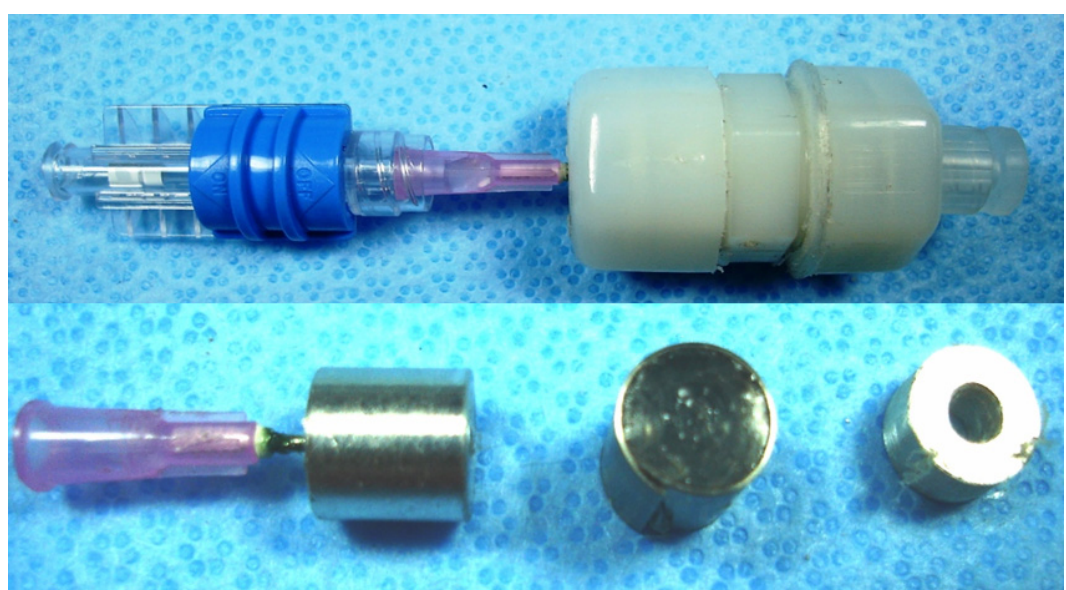


Figure 41: Second prototype of a hydrogel casting mould

Brass was chosen for its easiness of machining and resistance to corrosion. The discoloration on the specimen's surface could be the result of brass oxidation (Copper oxide is green). We believe that the extent of oxidation and subsequent staining of small areas on the specimen surface had no effect on the mechanical data collected from the specimen.

High pressures were encountered during cast injections. This made it impossible to use a conventional syringe for hydrogel injection. Therefore, the setup used a threaded rod and T-handle to provide the necessary axial mechanical advantage.

### 6.5.2 Hydrogel curing results

Dislodgment of the polypropylene plug at the vacuum end of the mould sometimes occurred during hydrogel injection. The injected hydrogel, gradually filling the mould, was expected to extrude through the small central hole of the polypropylene plug that was connected to the vacuum. However, the high hydrogel viscosity made it difficult for the hydrogel to vent through the central hole, but rather, the hydrogel pushed the polypropylene plug out of the brass tube. Cured specimen were

therefore sometimes not at a 1:1 height to diameter ratio. However, most still had flat surfaces perpendicular to the rotational axis of the specimen. Using a digital vernier caliper, the actually specimen height was recorded and subsequently used for strain calculation during axial compression.

# Chapter 7: Summary & Conclusions

To document the performance of an injectable in-situ PVA (poly vinyl alcohol) curing hydrogel as a nucleus replacement implant, specific experiments were designed, planned and successfully executed. The four parameters of the hydrogels that were identified to be crucial for a successful application were: swelling, stiffness, extrusion pressure and curing speed.

PVA121 and PVA14X used for the swelling experiments had uniform sizes and were tested after 14 days of incubation from its manufacturing date. Both hydrogels ultimately reached weight equilibrium at approximately 111 %. Weight loss of these hydrogels were not apparent within 8 wks of swelling for PVA121 (except for the last data point) and within 6 wks of swelling for PVA14X. Technical difficulties forced us to terminate the experiment with PVA14X at 7 weeks.

Stiffness of the PVA hydrogels were characterized over a period of 48 hrs, 4 wks and 8 wks after immersion in phosphate buffer saline (PBS) at 37 °C. Controls were tested at 0 hrs. PVA14X and PVA121 had, for low strain an average stiffness of 2.0 MPa and 1.5 MPa, respectively. Generally, stiffness increased by about 0.5 MPa over 4 weeks. This increase was considered insignificant for a practical application.

Extrusion pressures were found to be very time and temperature dependent. There is a possibility that the storage time of the hydrogels may also affect resultant extrusion pressures. Exponential regression analysis of plateau pressures showed reasonable data fits for temperature 25 °C, 37 °C, 50 °C and 60 °C. We conclude that an optimal working time of the hydrogel can easily be optimized by varying the injection temperatures.

Faster curing rates of PVA hydrogels suggest shorter resting periods for patients undergoing this hydrogel injection, nuclear pulposus replacement surgery. Results showed that PVA121 did not reach final

stiffness even after 2 weeks; whereas PVA14X cured much faster and reached 70% of its final stiffness after 72 hrs.

While this study showed promising results for the proprietary PVA hydrogel to be used for nuclear pulposus replacement, more work has to be done to further validate its suitability as a nuclear pulposus replacement candidate. Innate stability of the hydrogel over time, possible dissolution properties, long term fatigue and creep, post plasticity, elasticity and stiffness tolerances of the re-cured hydrogels are possible topics to continue this work.

# Bibliography

- [1] G. B. Andersson, "Epidemiology of low back pain," *Acta Orthop. Scand. Suppl*, vol. 281, pp. 28-31, June1998.
- [2] "Spinal implants: Accelerating growth, increasing competition,", MedPro Month VIII ed 1998.
- [3] N. Maniadakis and A. Gray, "The economic burden of back pain in the UK," *Pain*, vol. 84, no. 1, pp. 95-103, Jan.2000.
- [4] A. Carl, E. Ledet, H. Yuan, and A. Sharan, "New developments in nucleus pulposus replacement technology," *Spine J.*, vol. 4, no. 6 Suppl, pp. 325S-329S, Nov.2004.
- [5] N. A. Peppas, Y. Huang, M. Torres-Lugo, J. H. Ward, and J. Zhang, "Physicochemical foundations and structural design of hydrogels in medicine and biology," *Annu. Rev. Biomed. Eng*, vol. 2, pp. 9-29, 2000.
- [6] T. R. Oegema, Jr., "Biochemistry of the intervertebral disc," Clin. Sports Med., vol. 12, no. 3, pp. 419-439, July1993.
- [7] Yamada H., Strength of Biological Materials. Huntington, N.Y.: R.E. Krieger Pub. Co, 1973, p. 297.
- [8] W. Frobin, P. Brinckmann, M. Biggemann, M. Tillotson, and K. Burton, "Precision measurement of disc height, vertebral height and sagittal plane displacement from lateral radiographic views of the lumbar spine," *Clin. Biomech. (Bristol. , Avon. )*, vol. 12 Suppl 1, p. S1-S63, 1997.
- [9] S. P. Moroney, A. B. Schultz, J. A. Miller, and G. B. Andersson, "Load-displacement properties of lower cervical spine motion segments," *J. Biomech.*, vol. 21, no. 9, pp. 769-779, 1988.
- [10] A. L. Nachemson, A. B. Schultz, and M. H. Berkson, "Mechanical properties of human lumbar spine motion segments. Influence of age, sex, disc level, and degeneration," *Spine*, vol. 4, no. 1, pp. 1-8, Jan.1979.
- [11] M. Adams, N. Bogduk, K. Burton, and P. Dolan, *The biomechanics of back pain*, 2nd edition ed Elsevier Ltd, 2006.
- [12] J. C. latridis, M. Weidenbaum, L. A. Setton, and V. C. Mow, "Is the nucleus pulposus a solid or a fluid? Mechanical behaviors of the nucleus pulposus of the human intervertebral disc," *Spine*, vol. 21, no. 10, pp. 1174-1184, May1996.
- [13] Nachemson A. and Morris J.M., "In vivo measurements of intradiscal pressure discometry, a method for the determination of pressure in the lower lumbar discs," *J. Bone Joint Surg. Am*, vol. 46, pp. 1077-1092, July1964.
- [14] A. L. Nachemson, "Disc pressure measurements," *Spine*, vol. 6, no. 1, pp. 93-97, Jan.1981.
- [15] A. J. Lisi, C. W. O'Neill, D. P. Lindsey, R. Cooperstein, E. Cooperstein, and J. F. Zucherman, "Measurement of in vivo lumbar intervertebral disc pressure during spinal

- manipulation: a feasibility study," *J. Appl. Biomech.*, vol. 22, no. 3, pp. 234-239, Aug.2006.
- [16] N. Boos, A. Wallin, T. Gbedegbegnon, M. Aebi, and C. Boesch, "Quantitative MR imaging of lumbar intervertebral disks and vertebral bodies: influence of diurnal water content variations," *Radiology*, vol. 188, no. 2, pp. 351-354, Aug.1993.
- [17] R. J. Kowalski, L. A. Ferrara, E. C. Benzel, "Biomechanics of the Spine," *Neurosurg Q*, vol. 15, no. 1, pp. 42-59, 2005.
- [18] N. L. Nerurkar, D. M. Elliott, and R. L. Mauck, "Mechanics of oriented electrospun nanofibrous scaffolds for annulus fibrosus tissue engineering," *J. Orthop. Res.*, Apr.2007.
- [19] R. J. Moore, "The vertebral end-plate: what do we know?," *Eur. Spine J.*, vol. 9, no. 2, pp. 92-96, Apr.2000.
- [20] G. Waddell, "The epidemiology of back pain," in *The back pain revolution,* 2nd edn ed Elsevier limited, 2004, pp. 71-90.
- [21] J. P. Urban, S. Smith, and J. C. Fairbank, "Nutrition of the intervertebral disc," *Spine*, vol. 29, no. 23, pp. 2700-2709, Dec.2004.
- [22] T. Grunhagen, G. Wilde, D. M. Soukane, S. A. Shirazi-Adl, and J. P. Urban, "Nutrient supply and intervertebral disc metabolism," *J. Bone Joint Surg. Am*, vol. 88 Suppl 2, pp. 30-35, Apr.2006.
- [23] N. Boos, S. Weissbach, H. Rohrbach, C. Weiler, K. F. Spratt, and A. G. Nerlich, "Classification of age-related changes in lumbar intervertebral discs: 2002 Volvo Award in basic science," *Spine*, vol. 27, no. 23, pp. 2631-2644, Dec.2002.
- [24] P. J. Roughley, "Biology of intervertebral disc aging and degeneration: involvement of the extracellular matrix," *Spine*, vol. 29, no. 23, pp. 2691-2699, Dec.2004.
- [25] E. H. Cassinelli, R. A. Hall, and J. D. Kang, "Biochemistry of intervertebral disc degeneration and the potential for gene therapy applications," *The Spine Journal*, vol. 1, no. 3, pp. 205-214, 2001.
- [26] N. Bogduk, "Age changes in the lumbar spine," in *Clinical anatomy of the lumbar spine and sacrum,* 4th edn ed Elsevier Limited, 2007, pp. 165-171.
- [27] J. C. latridis, M. Weidenbaum, L. A. Setton, and V. C. Mow, "Is the nucleus pulposus a solid or a fluid? Mechanical behaviors of the nucleus pulposus of the human intervertebral disc," *Spine*, vol. 21, no. 10, pp. 1174-1184, May1996.
- [28] J. C. latridis, L. A. Setton, M. Weidenbaum, and V. C. Mow, "Alterations in the mechanical behavior of the human lumbar nucleus pulposus with degeneration and aging," *J. Orthop. Res.*, vol. 15, no. 2, pp. 318-322, Mar.1997.
- [29] J. P. Thompson, R. H. Pearce, M. T. Schechter, M. E. Adams, I. K. Tsang, and P. B. Bishop, "Preliminary evaluation of a scheme for grading the gross morphology of the human intervertebral disc," *Spine*, vol. 15, no. 5, pp. 411-415, May1990.
- [30] G. Waddell, "US health care for back pain," in *The back pain revolution* Elsevier limited, 2004, pp. 419-438.

- [31] D. J. Abraham, H. N. Herkowitz, and J. N. Katz, "Indications for thoracic and lumbar spine fusion and trends in use," *Orthop. Clin. North Am*, vol. 29, no. 4, p. 803, Oct.1998.
- [32] R. A. Deyo, A. Nachemson, and S. K. Mirza, "Spinal-fusion surgery the case for restraint," *N. Engl. J. Med.*, vol. 350, no. 7, pp. 722-726, Feb.2004.
- [33] P. Fritzell, O. Hagg, P. Wessberg, and A. Nordwall, "2001 Volvo Award Winner in Clinical Studies: Lumbar fusion versus nonsurgical treatment for chronic low back pain: a multicenter randomized controlled trial from the Swedish Lumbar Spine Study Group," *Spine*, vol. 26, no. 23, pp. 2521-2532, Dec.2001.
- [34] S. Etebar and D. W. Cahill, "Risk factors for adjacent-segment failure following lumbar fixation with rigid instrumentation for degenerative instability," *J. Neurosurg.*, vol. 90, no. 2 Suppl, pp. 163-169, Apr.1999.
- [35] J. C. Eck, S. C. Humphreys, and S. D. Hodges, "Adjacent-segment degeneration after lumbar fusion: a review of clinical, biomechanical, and radiologic studies," *Am J. Orthop.*, vol. 28, no. 6, pp. 336-340, June1999.
- [36] M. N. Kumar, A. Baklanov, and D. Chopin, "Correlation between sagittal plane changes and adjacent segment degeneration following lumbar spine fusion," *Eur. Spine J.*, vol. 10, no. 4, pp. 314-319, Aug.2001.
- [37] T. J. Errico, "Why a mechanical disc?," Spine J., vol. 4, no. 6 Suppl, pp. 151S-157S, Nov.2004.
- [38] C. K. Lee and V. K. Goel, "Artificial disc prosthesis: design concepts and criteria," *Spine J.*, vol. 4, no. 6 Suppl, pp. 209S-218S, Nov.2004.
- [39] S. P. Leary, J. J. Regan, T. H. Lanman, and W. H. Wagner, "Revision and explantation strategies involving the CHARITE lumbar artificial disc replacement," *Spine*, vol. 32, no. 9, pp. 1001-1011, Apr.2007.
- [40] C. D. Ray, "The PDN prosthetic disc-nucleus device," Eur. Spine J., vol. 11 Suppl 2, p. S137-S142, Oct.2002.
- [41] L. G. Griffith and G. Naughton, "Tissue engineering-current challenges and expanding opportunities," *Science*, vol. 295, no. 5557, pp. 1009-1014, Feb.2002.
- [42] G. Paesold, A. G. Nerlich, and N. Boos, "Biological treatment strategies for disc degeneration: potentials and shortcomings," *Eur. Spine J.*, vol. 16, no. 4, pp. 447-468, Apr.2007.
- [43] Martino A.D., Vaccaro A.R., Lee J.Y., Denaro V., and Lim M.R., "Nucleus pulposus replacement: basic science and indications for clinical use," *Spine*, vol. 30, no. 16 Suppl, p. S16-S22, Aug.2005.
- [44] "NUBAC™ Pioneer Surgical Technology, Inc.," 2004.
- [45] A. N. Sieber and J. P. Kostuik, "Concepts in nuclear replacement," *Spine J.*, vol. 4, no. 6 Suppl, pp. 322S-324S, Nov.2004.
- [46] R. Bertagnoli, C. T. Sabatino, J. T. Edwards, G. A. Gontarz, A. Prewett, and J. R. Parsons, "Mechanical testing of a novel hydrogel nucleus replacement implant," *Spine J.*, vol. 5, no. 6, pp. 672-681, Nov.2005.

- [47] Peterson L., "Trends-in-Medicine," 2008.
- [48] Biomet Incorporated (BMET), "Biomet F1Q07 (Qtr End 8/31/06) Earnings Call Transcript (SeekingAlpha)," 2006.
- [49] Buttermann G.R. and Beaubien B.P., "Stiffness of prosthetic nucleus determines stiffness of reconstructed lumbar calf disc," *Spine J.*, vol. 4, no. 3, pp. 265-274, May2004.
- [50] I. Disc Dynamics, "DASCOR," 2007.
- [51] "CryoLife's BioDisc(TM) Nucleus Pulposus Replacement to be Featured at Two Medical Conferences in Berlin," 2007.
- [52] A. Joshi, G. Fussell, J. Thomas, A. Hsuan, A. Lowman, A. Karduna, E. Vresilovic, and M. Marcolongo, "Functional compressive mechanics of a PVA/PVP nucleus pulposus replacement," *Biomaterials*, vol. 27, no. 2, pp. 176-184, Jan.2006.
- [53] J.Li, "Polymeric Hydrogels," in *Engineering Materials for Biomedical Applications*. H. Teoh Swee, Ed. 2004.
- [54] Schacht E.H., "Polymer chemistry and hydrogel systems," *Journal of Physics: Conference Series*, vol. 3, no. 2004, pp. 22-28, 2004.
- [55] A. S. Hoffman, "Hydrogels for biomedical applications," *Ann. N. Y. Acad. Sci.*, vol. 944, pp. 62-73, Nov.2001.
- [56] C.M.Hassan and N.A.Peppas, "Structure and Applications of Poly(vinyl alcohol) hydrogels produced by conventional crosslinking or by freezing/thawing methods," in *Advances in Polymer Science* Springer Berlin / Heidelberg, 2000, pp. 37-65.
- [57] J. M. Cloyd, N. R. Malhotra, L. Weng, W. Chen, R. L. Mauck, and D. M. Elliott, "Material properties in unconfined compression of human nucleus pulposus, injectable hyaluronic acid-based hydrogels and tissue engineering scaffolds," *Eur. Spine J.*, July2007.
- [58] E. J. Boelen, L. H. Koole, L. W. van Rhijn, and C. S. van Hooy-Corstjens, "Towards a functional radiopaque hydrogel for nucleus pulposus replacement," *J. Biomed. Mater.* Res. B Appl. Biomater., Apr.2007.
- [59] R. Bertagnoli, C. T. Sabatino, J. T. Edwards, G. A. Gontarz, A. Prewett, and J. R. Parsons, "Mechanical testing of a novel hydrogel nucleus replacement implant," *Spine J.*, vol. 5, no. 6, pp. 672-681, Nov.2005.
- [60] E. J. Boelen, C. S. van Hooy-Corstjens, S. K. Bulstra, O. A. van, L. W. van Rhijn, and L. H. Koole, "Intrinsically radiopaque hydrogels for nucleus pulposus replacement," *Biomaterials*, vol. 26, no. 33, pp. 6674-6683, Nov.2005.
- [61] J. Vernengo, G. W. Fussell, N. G. Smith, and A. M. Lowman, "Evaluation of novel injectable hydrogels for nucleus pulposus replacement," *J. Biomed. Mater. Res. B Appl. Biomater.*, Apr.2007.
- [62] J. K. Katta, M. Marcolongo, A. Lowman, and K. A. Mansmann, "Friction and wear behavior of poly(vinyl alcohol)/poly(vinyl pyrrolidone) hydrogels for articular cartilage replacement," *J. Biomed. Mater. Res. A*, vol. 83, no. 2, pp. 471-479, Nov.2007.

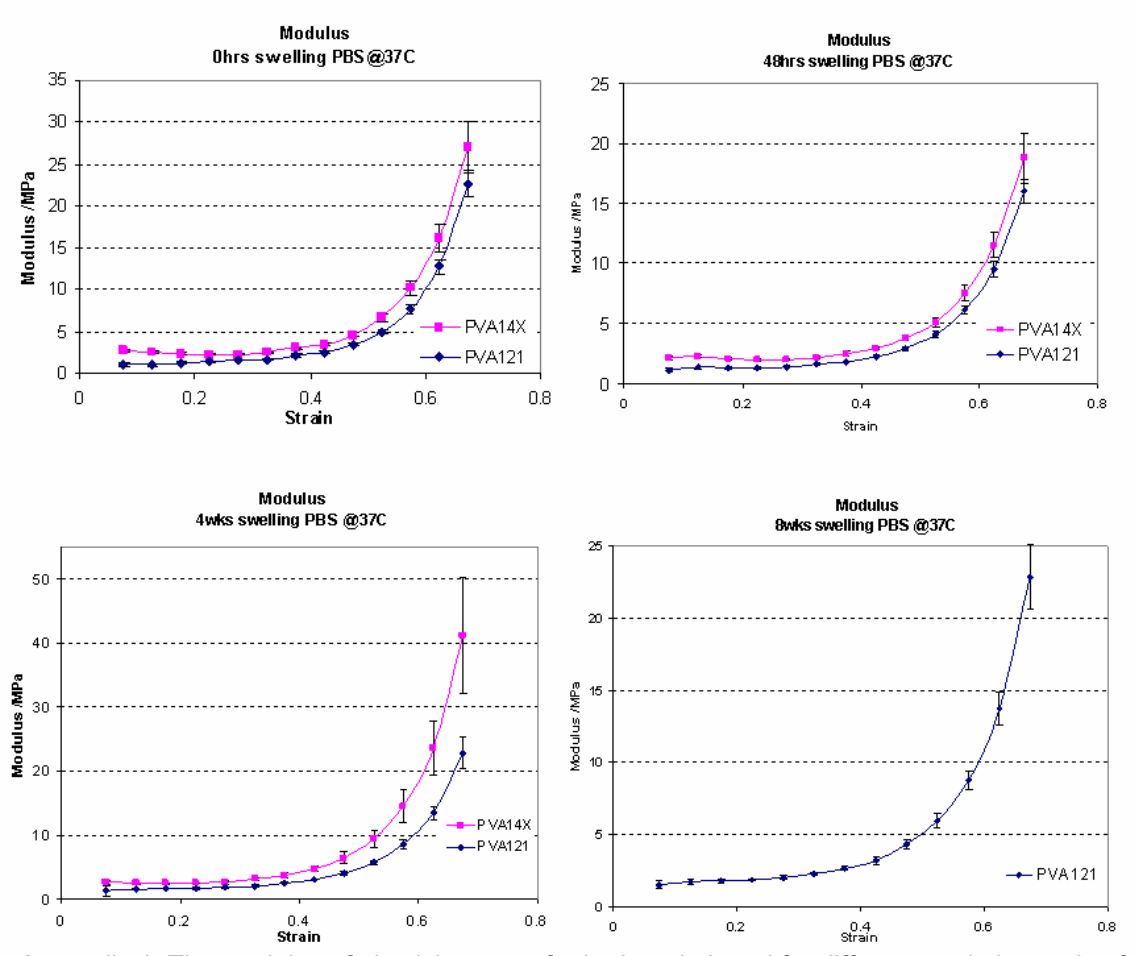
- [63] P. H. Corkhill, A. S. Trevett, and B. J. Tighe, "The potential of hydrogels as synthetic articular cartilage," *Proc. Inst. Mech. Eng [H. ]*, vol. 204, no. 3, pp. 147-155, 1990.
- [64] Y.Waknine, "International Approvals: Arctic Front, RealTime HCV, Dascor Disc," 2005.
- [65] P. M. Klara and C. D. Ray, "Artificial nucleus replacement: clinical experience," *Spine*, vol. 27, no. 12, pp. 1374-1377, June2002.
- [66] Q. B. Bao and P. A. Higham, "Hydrogel intervertebral disc nucleus,"**United States Patent** 5,976,186, Feb.11, 1999.
- [67] Q. B. Bao and P. A. Higham, "Hydrogel intervertebral disc nucleus with diminished lateral bulging," **United States Patent** 5,534,028, Sept.7, 1996.
- [68] Q. B. Bao and P. A. Higham, "Hydrogel bead intervertebral disc nucleus," United States Patent 5,192,326, Sept.3, 1993.
- [69] Q. B. Bao and P. A. Higham, "Hydrogel intervertebral disc nucleus,"**United States Patent** 5,047,055, Oct.9, 1991.
- [70] Q. B. Bao and H. A. Yuan, "Artificial disc technology," *Neurosurg. Focus.*, vol. 9, no. 4, p. e14, 2000.
- [71] J. A. Stammen, S. Williams, D. N. Ku, and R. E. Guldberg, "Mechanical properties of a novel PVA hydrogel in shear and unconfined compression," *Biomaterials*, vol. 22, no. 8, pp. 799-806, Apr.2001.
- [72] M. J. Allen, J. E. Schoonmaker, T. W. Bauer, P. F. Williams, P. A. Higham, and H. A. Yuan, "Preclinical evaluation of a poly (vinyl alcohol) hydrogel implant as a replacement for the nucleus pulposus," *Spine*, vol. 29, no. 5, pp. 515-523, Mar.2004.
- [73] J. Thomas, A. Lowman, and M. Marcolongo, "Novel associated hydrogels for nucleus pulposus replacement," *J. Biomed. Mater. Res. A*, vol. 67, no. 4, pp. 1329-1337, Dec.2003.
- [74] M. Marcolongo and A. Lowman, "Associating hydrogels for nucleus pulposus replacement in intervertebral discs," Aug.5, 2007.
- [75] A. A. White and M. M. Panjabi, *Clinical Biomechanics of the Spine*, 2 ed Lippincott Williams & Wilkins, 1990.
- [76] D. J. Botsford, S. I. Esses, and D. J. Ogilvie-Harris, "In vivo diurnal variation in intervertebral disc volume and morphology," *Spine*, vol. 19, no. 8, pp. 935-940, Apr.1994.
- [77] H. J. Wilke, P. Neef, M. Caimi, T. Hoogland, and L. E. Claes, "New in vivo measurements of pressures in the intervertebral disc in daily life," *Spine*, vol. 24, no. 8, pp. 755-762, Apr.1999.
- [78] K. Sato, S. Kikuchi, and T. Yonezawa, "In vivo intradiscal pressure measurement in healthy individuals and in patients with ongoing back problems," *Spine*, vol. 24, no. 23, pp. 2468-2474, Dec.1999.
- [79] A. T. Trout, D. F. Kallmes, K. F. Layton, K. R. Thielen, and J. G. Hentz, "Vertebral endplate fractures: an indicator of the abnormal forces generated in the spine after vertebroplasty," *J. Bone Miner. Res.*, vol. 21, no. 11, pp. 1797-1802, Nov.2006.

- [80] A. Gloria, F. Causa, S. R. De, P. A. Netti, and L. Ambrosio, "Dynamic-mechanical properties of a novel composite intervertebral disc prosthesis," *J. Mater. Sci. Mater. Med.*, July2007.
- [81] E. Y. Ng and L. T. Chua, "Prediction of skin burn injury. Part 2: Parametric and sensitivity analysis," *Proc. Inst. Mech. Eng [H. ]*, vol. 216, no. 3, pp. 171-183, 2002.
- [82] F. P. Lees, "Fire," in Loss Prevention in the Process Industries: Hazard Identification, Assessment and Control Butterworth-Heinemann, 1996, pp. 246-249.

# Appendix

Appendix 1: The modulus of elasticity range for hydrogel plotted for different strain intervals of	
unconfined compression	90
Appendix 2: Numerical tabulation of PVA121 and PVA14X modulus of elasticity	91

# Appendix



Appendix 1: The modulus of elasticity range for hydrogel plotted for different strain intervals of unconfined compression

	D\/A404			DVA44V	1	
PVA121			PVA14X			
	C @ 10-20 % Strain	OTDE) (	T: "	25 °C @ 10-20 % Strain	OTDE) /	
Time /hrs	Stiffness /MPa		Time /hrs	Stiffness /MPa	STDEV	
8	0.1	0.1	2	0.2	0.1	
24	0.1	0.1	8	0.4	0.1	
72	0.4	0.1	24	1.3	0.2	
168	1.0	0.1	72	1.9	0.2	
336	1.3	0.1	336	2.7	0.3	
25 °C @ 20-30% Strain		25 °C @ 20-30% Strain				
Time /hrs	Stiffness /MPa	STDEV	Time /hrs	Stiffness /MPa	STDEV	
8	0.1	0.1	2	0.3	0.1	
24	0.2	0.0	8	0.6	0.1	
72	0.5	0.1	24	1.4	0.2	
168	1.1	0.1	72	2.0	0.1	
336	1.4	0.1	336	2.9	0.4	
37 <sup>°</sup> C @ 10-20 % Strain			37 $^{\circ}$ C @ 10-20 % Strain			
Time /hrs	Stiffness /MPa	STDEV	Time /hrs	Stiffness /MPa	STDEV	
8	0.1	0.0	2	0.2	0.0	
24	0.0	0.1	8	0.5	0.0	
72	0.5	0.0	24	1.6	0.2	
168	1.4	0.2	72	2.5	0.3	
336	1.9	0.1	336	2.9	0.3	
37 <sup>C</sup>	C @ 20-30% Strain	•	37 °C @ 20-30% Strain			
Time /hrs	Stiffness /MPa	STDEV	Time /hrs	Stiffness /MPa	STDEV	
8	0.0	0.1	2	0.2	0.1	
24	0.2	0.1	8	0.7	0.1	
72	0.7	0.1	24	1.8	0.2	
168	1.5	0.2	72	2.1	0.1	
336	1.9	0.1	336	3.2	0.3	
50 °	C @ 10-20 % Strain	•	50C °C @ 10-20 % Strain			
Time /hrs	Stiffness /MPa	STDEV	Time /hrs	Stiffness /MPa	STDEV	
8	0.1	0.1	2	0.1	0.1	
24	0.0	0.1	8	0.4	0.2	
72	0.6	0.1	24	1.3	0.1	
168	1.2	0.2	72	1.8	0.1	
336	1.5	0.1	336	2.5	0.3	
	C @ 20-30% Strain	1 211		50 °C @ 20-30% Strain		
Time /hrs	Stiffness /MPa	STDEV	Time /hrs	Stiffness /MPa	STDEV	
8	0.0	0.1	2	0.1	0.0	
24	0.0	0.1	8	0.6	0.1	
72	0.7	0.1	24	1.3	0.1	
168	1.4	0.1	72	1.8	0.2	
336	1.7	0.2	336	3.1	0.3	
330	CONTROL			CONTROL		
Time /hrs	Stiffness /MPa	STDEV	Time /hrs	Stiffness /MPa	STDEV	
336	2.3	0.1	336	2.7	0.2	
336	2.3	0.1	336	3.1	0.2	
				PVA14X modulus of elastic		

Appendix 2: Numerical tabulation of PVA121 and PVA14X modulus of elasticity